IEEE Access
Multidisciplinary ⋮ Rapid Review ⋮ Open Access Journal

Received 18 November 2023, accepted 28 November 2023, date of publication 30 November 2023,
date of current version 6 December 2023.

Digital Object Identifier 10.1109/ACCESS.2023.3338164

TOPICAL REVIEW

A Comprehensive Review on Single-Stage WPT Converter Topologies and Power Factor Correction Methodologies in EV Charging

D. PURUSHOTHAMAN[1], R. NARAYANAMOORTHI[1], (Member, IEEE), ALI ELRASHIDI[2,3], AND HOSSAM KOTB[4]

[1]Department of Electrical and Electronics Engineering, SRM Institute of Science and Technology, Kattankulathur, Chennai 603203, India
[2]Electrical Engineering Department, University of Business and Technology, Ar Rawdah, Jeddah 23435, Saudi Arabia
[3]Engineering Mathematics Department, Faculty of Engineering, Alexandria University, Alexandria 21544, Egypt
[4]Department of Electrical Power and Machines, Faculty of Engineering, Alexandria University, Alexandria 21544, Egypt

Corresponding authors: R. Narayanamoorthi (narayanamoorthi.r@gmail.com) and Ali Elrashidi (a.elrashidi@ubt.edu.sa)

This work was supported in part by the Government of India, Department of Science and Technology (DST), Science and Engineering Research Board (SERB) Core Research under Grant CRG/2020/004073.

ABSTRACT Wireless Power Transfer (WPT) particularly in the field of Electric Vehicle charging applications has wide research opportunities because of its huge growth. The power transfer efficiency is of major concern and researchers are finding ways to improve it by reducing stages of the WPT and making it better than the wired EV charging method. The increasing penetration of charging stations in the grid brings many challenges and hence to find a suitable control scheme to enhance input power quality. For the most optimal operation and comprehensive support, the charging systems must incorporate a suitable converter topology, a well-defined control strategy, and comply with all relevant grid codes and standards. For smooth and efficient functioning these features must be included in the EV charging systems. This paper presents a review of single-stage topologies and the power factor correction methods employed for EV wireless charging. An overview of different charging methods is first presented then the AC input and DC input single-stage converter are discussed, and following that methodologies for improving power factor correction are reviewed with the comparative analysis from different literatures. Finally, the challenges in single-stage wireless power transfer (SSWPT) were addressed and the future scopes were discussed which provides the future research directions.

INDEX TERMS EV charging, power factor correction, single-stage converter, WPT.

I. INTRODUCTION

The Electric Vehicle (EV) has drawn more attention in recent years. The EV industry's growth is vast in the search for a substitute to traditional Internal Combustion Engine (ICE) vehicle transportation during the era of the increase in fuel prices [1]. Transportation contributes a major part to the growth of the economy and adversely it contributes as a prime source of Greenhouse gas emissions. Depending only on ICE vehicles for transportation impacts the growth during times of increase in fuel prices. Hence as an alternative to ICE transportation EVs can be chosen to take part in transportation electrification and decarbonization as well [2]. Over the years carbon dioxide emission around the globe tends to increase exponentially resulting in the global temperature rise which creates adverse effects [3], [4]. This impacted the governments to invest in clean energy [5] rather than fossil fuels. The International Energy Agency (IEA) lays out Net Zero by 2050 Scenario [6] and suggests shifting to clean energy sources such as solar, wind and low-emission fuels, and transport electrification. Shifting towards renewable energy in making completely emission-free and clean energy-powered EVs, the California Air Resources Board (CARB) initiated a long-term goal of the emission-free vehicle program by laying the regulations for vehicle manufacturers aimed to achieve by 2035 [7]. In the trend curve [8] Fig. 1. it is clearly

The associate editor coordinating the review of this manuscript and approving it for publication was Alon Kuperman.

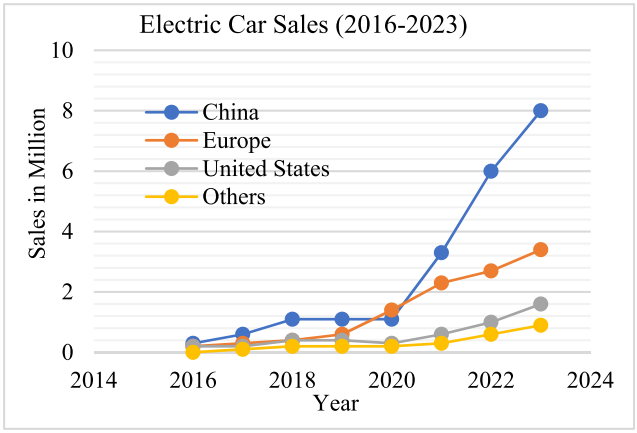

FIGURE 1. Electric car sales during (2016-2023).

evident that the year-wise EV sales increase and have a wide opportunity for EV growth. The advancements in semiconductor technologies, battery technologies and foremost the government's immersion have brought the EV industry to the next level. Owing to the high price of EVs compared to ICEs [9] and poor charging infrastructure people preferred fuel-powered vehicles in the early 19th century and now the emerging newer technologies tend people to prefer EVs. The broad classification of electric vehicles gives the types battery EV (BEV), fuel cell EV (FCEV), Plug-in hybrid EV (PHEV) and Hybrid EV (HEV) and Fig. 2 (a-d) Gives the structure of various types of EVs. BEV is entirely dependent on the battery source and is emission-free with the driving range depending on the battery capacity installed. The diagrammatic representation of BEV is shown in Fig. 2 (a). PHEV is comprised of ICE and an electric motor which can run until the battery power drains and shifts to ICE mode. The PHEV structure is given in Fig. 2 (b). Here battery charging can be done in both regenerative and plug-in modes. HEV has a similar operation as that of PHEV but plug-in charging is absent in this type and only the regenerative method charges the battery. The conceptual diagram of HEV is given in Fig. 2 (c). The main source of energy for FCEV is hydrogen which is used to generate electricity to run the motor and is completely emission-free and is given in Fig. 2 (d). Table 1. gives the comparison of features between ICE, BEV, PHEV, HEV and FCEV. The major limitations [3], [9] of EVs are limited driving range and battery life, expensive battery cost, long charging time and charging compatibility issues.

The driving range limitations shall be overcome by the implementation of fast charging, ultrafast charging stations and laying dynamic charging lanes [10], [11], [12], [13]. Refueling the ICE is very quick compared to EV battery charging and hence efficient quick charging methods are required to overcome the long charging times. Even though fast chargers charge the battery quickly, battery life gets depleted by the use of fast chargers and hence adaptive battery charging methods can be utilized to extend the life of Li-on batteries during the charging of EVs [12], [14]. The rating of the battery differs from vehicle to vehicle requiring the EV charging stations to facilitate the wide range operation. The evolution of advanced battery technology and the installation of new charging centers with robust controllers makes people prefer EVs which leads to the growth of the EV industry. According to IEA [15], Globally there were more than 2.7 million charging points installed till the year 2022, from this over 900,000 centers of them have been installed within the same year with more than 600000 public slow charging points. China is a leader in installing public charging points with 360000 slow charging centers and 330000 fast charging centers in the year 2022. The development of the EV sector brings the necessity of implementing the charging standards for EVs around the world for the charging structure infrastructure interaction [10]. In the standardizations of charging and grid integration, the Institute of Electrical and Electronics Engineers (IEEE) and the Society of Automotive Engineers (SAE) contributes an important role. The widely used standards for EV charging are International Electro-technical Commission (IEC) and SAE while the former is established by a British standard organization and the latter is established by a US professional body [3], [5], [10], [16], [17]. Various standards available with their purposes are given in Table 2. Unlike conventional ICE vehicles, BEVs require additional safety measures to be set as they contain Li-ion batteries and have the risk of fire [18]. The National Fire Protection Association (NFPA) guides in establishing NFPA 70 standards [19] and the National Electric Code (NEC) specifies the NEC 625 standards [20] to adopt safety measures. The battery management system is essential for a BEV in managing and monitoring the health and safety conditions of the battery. Designing a fail-safe battery management system (BMS) to eliminate the safety risks in the battery is a challenging part. Battery technology and charging technology are the two essential factors that influence the growth of the EV industry apart from other factors that influence indirectly like vehicle cost, fuel price hikes, government policies, environmental conditions and global trends. Hence a survey on one essential factor i.e., charging technology is carried out in this work.

The limitations in current EV charging converters have to be identified and improvements have to be made in EV charging technologies. The organization of the review paper consists of an outline of charging technologies for EVs in section II, a discussion of SSWPT articles with their proposed circuit in section III, a discussion of Power factor correction technologies and their control methods for the SSWPT in section IV, challenges faced in implementing SSWPT technologies is discussed in section V, the scope for future work in the emerging charging technologies is discussed in section VI and the conclusions found from the review of the SSWPT is presented in section VII.

II. EV CHARGING TECHNOLOGIES

Charging plays a significant role in the growth of the EV sector as the charging time and range of travel depend on charger capacity and the rating of the battery installed and the

TABLE 1. Comparison between ICE, BEV, PHEV, HEV and FCEV.

Characteristics	ICE [21], [22]	BEV [23], [24]	PHEV [25], [26]	HEV [27], [28]	FCEV [29], [30]
Propulsion Device	ICE	Electric Motor	Electric Motor and ICE	Electric Motor and ICE	Electric Motor
Source of Energy	Fuel	Battery	Battery and Fuel	Fuel	Fuel Cell
Efficiency	Low	High	Moderate	Moderate	High
Fueling/Charging time	Less	More	More	Less	Less
CO2 Emission	Maximum	No	Very Less	Less	No
Vehicle Cost	Less	High	High	Moderate	High
Life Span	Long	Short	Long	Long	Short
Maintenance	Less	Very less	More	More	More
Service availability	More	Moderate	Moderate	Moderate	Less
Advantages	Driving range, Energy efficient	Maintenance Free, Energy efficient	Hybrid, Driving range, Economic	Regenerative energy support	High efficiency, Economic
Limitations	Gasoline Price dependent	High Cost, Charging Time, BMS	Complex Structure	Reduced efficiency in battery mode	Fueling station, Complex Structure

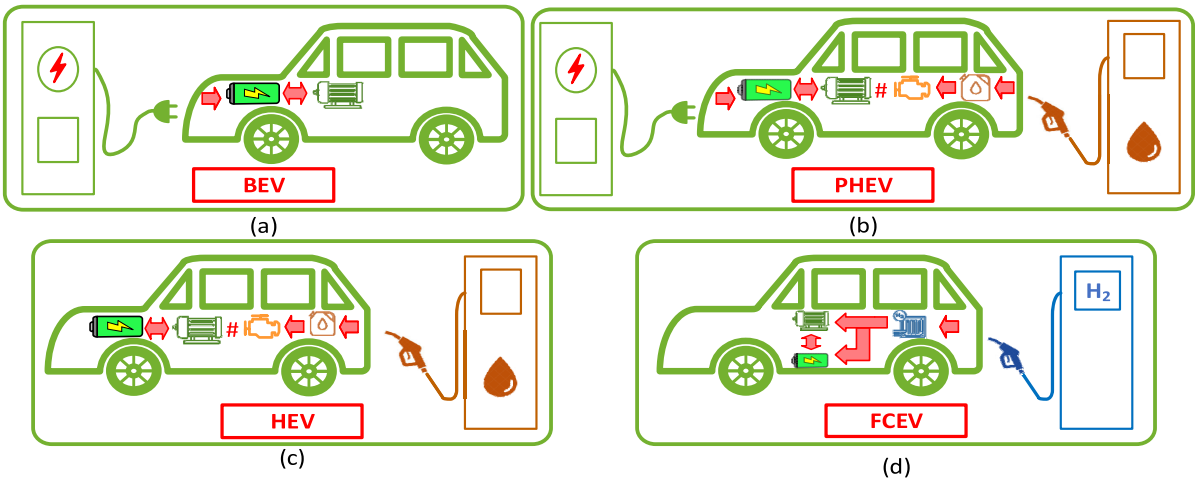

FIGURE 2. Types of EV structures. (a) BEV (b) PHEV (c) HEV (d) FCEV.

cost increases if battery capacity is increased [11], [17], [31]. EV charging can be commonly classified into wired, wireless and hybrid charging systems. The Common BEV charging methods are represented in Fig. 3 (a-d). The first method of charging is wired charging [32], [33], [34], [35], [36], [37], [38], [39], [40], [41], [42], [43] which has AC and DC types with non-isolated [32], [33], [34], [35] and isolated [36], [37], [38], [39], [40], [41], [42], [43] methods of charging structures and has the benefits of the highest efficiency due to the conductive mode of charging with the drawback of specific cable and connector requirements. The Second method is wireless EV charging [44], [45], [46], [47], [48], [49], [50], [51], [52], [53], [54], [55] which offers a safe and comprehensible charging structure with inherent grid isolation and reduces the battery capacity in the case of a dynamic charging environment. The third method is hybrid EV charging [56], [57], [58], [59], [60], [61], [62], [63] which combines the features of both the wired and wireless methods of charging with the use of shared converters or dedicated converters for wired and wireless modes of charging. Problems such as high cost, big size, poor performance and low power level can be overcome by integrating wireless/wired and fast charging methods. Another method employed as an alternative for EV charging is the battery swapping (BS) method [64], [65], [66], [67], [68], [69] in which the discharged battery is instantly replaced by the same kind of charged battery at the battery swapping station (BSS) and has the drawback of high rental charges and huge investment for the BSS proprietors. Table 3 shows the comparison of BEV charging methods for wired, wireless, hybrid and BS methods. EV charging can also

TABLE 2. Organization and defined standards related to EV charging.

Organization	Country	Standards Defined
Institute of Electrical and Electronics Engineers (IEEE)	United States	• Harmonic Control standards • Power quality standards • Radiofrequency Emission measurement in WPT • Smart grid interoperability standards
Society of Automotive Engineers (SAE)	United States	• Supply requirements for EV • Conductive Charging Standards • Wireless Charging Standards • Communication standards • Safety and testing requirements
International Electro-technical Commission (IEC)	Britain	• Battery safety, testing and maintenance • Converters design control and maintenance • Installation, Protection and safety requirements • Charging Requirements, • WPT standards • Sockets, Plugs and Connectors standards
CHArge de MOve (CHAdeMo)	Japan	• Charging plugs and sockets standards • EV Battery Testing and characterization standards • Contactless and quick charging standards
Underwriters Laboratories (UL)	United States	• Protection requirements for EV charging • Supply, charging and plug-socket requirements • Inverter, converter and charge controller requirements for safety and grid stability
National Fire Protection Association (NFPA) and National Electric Code (NEC)	USA	• Safety measures for grid integration and equipment maintenance. • Workplace safety standards • Off-board charging standards • Charging infrastructure standards
Deutsches Institut fuer Normung (DIN)	Germany	• Battery standards and battery testing standards • Charging cable standards
Standardization Administration of China (SAC)	China	• Conductive charging standards and general requirements • EMC standards for Electric Vehicle Supply Equipment • Onboard conductive charging standards • Off-board communication protocol and BMS standards • Infrastructure standards for EV charging and Battery swapping • Decentralized EV charging facility standards • Charging station design standards

be classified according to the power levels by SAE J1772 standard as level I, level II and level III also termed as Fast charging (DC) [70], [71]. A comparison table is presented in Table 4. summarizing the three power levels with their range, operating voltage, charging time, place of use and connectors utilized.

A. WIRED CHARGING

Wired charging is given in Fig. 3 (a) commonly called conductive charging [72] requires a power cable of a specific standard to connect the grid and the EV in charging the battery with better efficiency. In recent years, high-gain DC/DC converters [33], [34] have garnered significant interest and attention in various industries. These converters offer distinct advantages in terms of their ability to deliver higher output voltages while minimizing power loss. Various capabilities are extended for conductive charging by incorporating suitable methodologies to provide continuous load current, reduce switching stress on the converter switches, bidirectional capability [35], increased current capability [36], combined slow and fast charging [37], improved power quality [38], extended output range [39], [40], high current density [41], wide voltage operation [42], input voltage-to-output current gain property [43], and other functions. Table 5. gives the summary of the topologies employed for wired charging of BEV with the converter rating and peak efficiency. The control methodology adopted in conductive charging also brings sufficient developments including enhancing controllability, fast operation, and multi-functional capability.

B. WIRELESS CHARGING

Because of several advantages rather than drawbacks WPT is preferred over other modes of charging EVs [73]. The foundation for WPT was laid over a decade ago by Nikola Tesla in the year 1899 who developed an experimental setup for the transmission of electric power over a distance of 24 miles wirelessly [74]. Later in the middle of the nineteenth century, WPT was not given more importance and after the advancement in the power electronics sector, it rose again and implemented near-field WPT technologies [75], [76] for smaller appliances.

The significant improvement resulted in the development of WPT charger companies and was applied for high-power applications [77], [78], [79], [80], [81]. Wireless charging at present lies in the research and development stage and has been applied in several applications such as mobile charging, robotics, medical implants, drones, EV charging etc. [82]. The functional diagram of wireless charging is shown in Fig. 3 (b). As an application for EV charging, it offers versatile features like galvanic isolation, charging on the go and battery capacity reduction [83], [84], [85], [86]. Wireless charging can be subdivided into static, dynamic and quasi-dynamic methods. The static WPT method [44], [45], [46], [47], [48] is employed when the vehicle stands stationary and has better efficiency and control than the other two

TABLE 3. BEV charging methods comparison.

Charging Method	Advantages	Limitations	Efficiency
Wired [32]–[43]	Higher charging efficiency Easy charging method.	Specific Charger and socket requirements Electric shock hazards Vehicles need to be stationary throughout the charging period.	Very high
Wireless [44]–[55]	High electrical isolation Increased safety Convenient and easy method of charging.	Slow charging Charging pad Misalignment problem Complex control Electromagnetic Interference problem.	Low
Hybrid [56]–[63]	Convenient charging Dual (Wireless/Wired) charging mode.	Increased cost Complex control	High
BS [64]–[69]	Easy and quick Charging method (Battery replacement) Increased battery life	An identical battery is required for the swap High investment Manpower required Difficult in battery swap for Heavy vehicles.	High

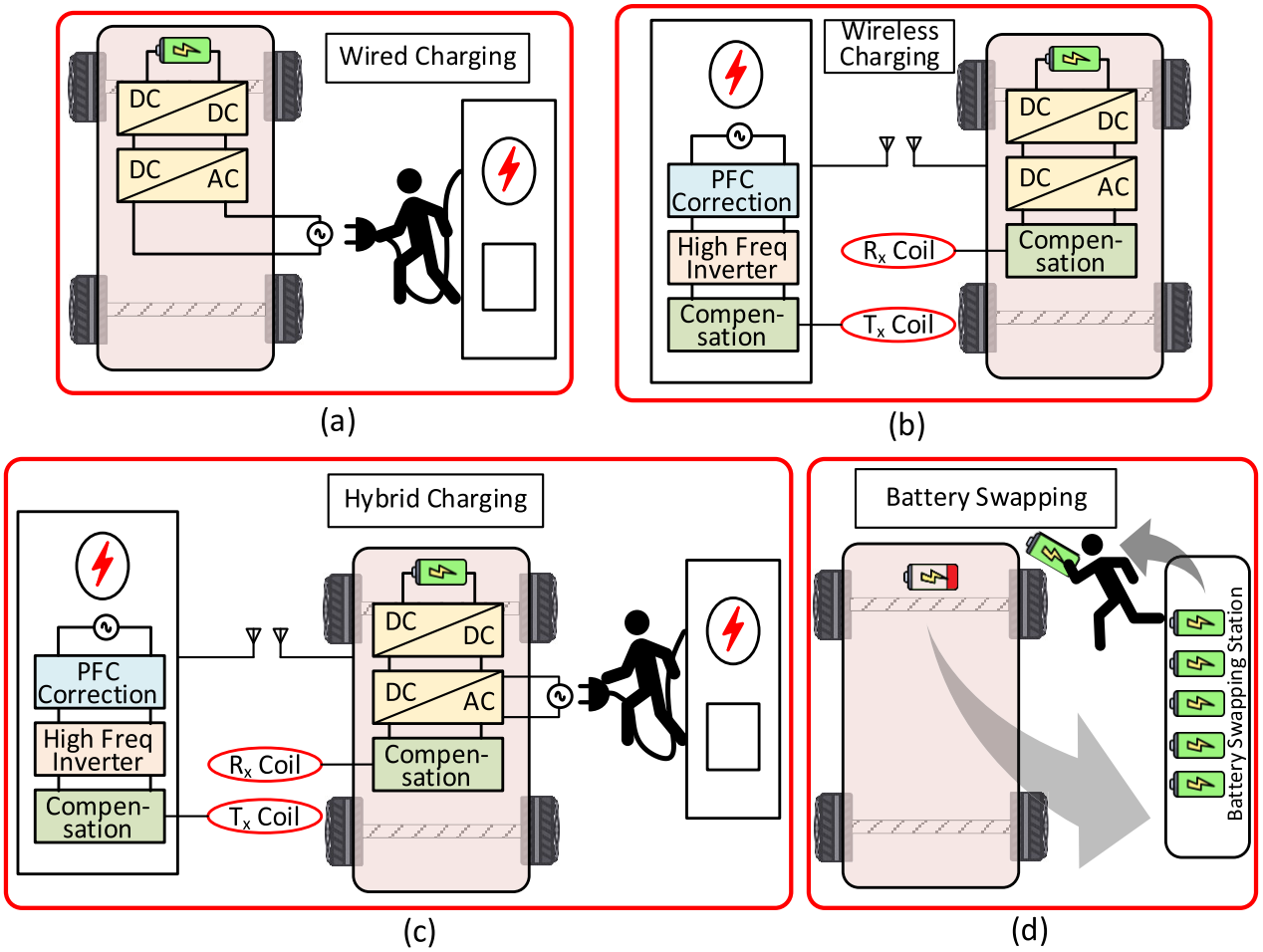

FIGURE 3. BEV charging Methods (a) Wired Charging (b) Wireless Charging (c) Hybrid Charging (d) Battery Swapping.

methods. The charging time relies on factors like the level of power source, charging pad size, design [87], [88] and distance between them. Static WPT can be installed at residential locations, parking stations, commercial buildings and shopping centers. In dynamic WPT [49], [50], [51], [52], [53], the charging while driving concept is applicable by laying a separate charging lane over which the moving vehicle can be charged. Since the vehicle is moving, misalignment

TABLE 4. BEV charging levels comparison.

Charging Level	Operating Voltage	Power Level	EV range in miles per hour	Charging Time	Full charge Cost	Place of installation	Connector Type
Level 1 (AC)	120 V	1.3-2.4 KW	3-5	Slow (24 Hours)	$1.20-$6.00	Residential	NEMA 5-15
Level 2 (AC)	208-240 V	3-19 KW	18-28	Medium (< 8 Hours)	$6.00-$10.00	Workplace	J1772, Type 2
Level 3 (DC Fast Charge)	208-480V	25-350 KW	> 100	Fast (60-90 Mins)	$10.00 to $30.00	Public	CHAdeMO, CCS, Tesla Supercharger

TABLE 5. Wired charging topologies comparison.

Topology	Rating (W)	Freq (kHz)	Switches	Diodes	HF Transformer	Efficiency (%)
Buck-Boost Converter[32]	100	10	3	2	0	98.2
Z quasi-resonant DC/DC Converter[33]	300	20	8	1	0	91.5
Modified buck-boost Converter[34]	500	50	9	0	0	97.2
Buck-Boost Converter[35]	3,800	25	12	1	0	87.2
Dual Active Bridge Converter[36]	20,000	10	18	0	3	94.8
Dual Active Bridge Converter[37]	5,000	100-220	8	4	1	98.2
Modified Bridgeless Luo converter[38]	850	20	3	3	1	90.8
Full Bridge Converter[39]	500	60	5	6	1	97.5
Full Bridge Converter[40]	10,000	85-337	4	8	2	98.5
Interleaved Boost Converter[41]	-	15.5	4	6	1	-
Full Bridge Converter[42]	11,000	15	7	8	1	98.3
Stacked half-bridge Converter[43]	6,600	500	8	0	1	98.2

becomes a major problem, which needs to be addressed by suitable compensation [89], [90], [91] to maximize the transfer efficiency. This method can be employed on the highways by installing a series of coils on a specific charging track. Quasi-dynamic WPT [54], [55] is similar to dynamic WPT but here the vehicle is not continuously moving but limited relative movement makes this to have this name and is installed at traffic signals where the vehicle stops for a short duration. In literature [44] a control strategy with three closed loops is employed to operate the WPT system at any point within the Optimal Operating Frequency Range and to dynamically tune the phase shift and frequency, ensuring that the designed system always operates at the preset ZVS angle with the desired output. A 500W Prototype was developed for testing with a coupling factor of k=0.2 and achieved a peak overall efficiency of 94.9%. An enhanced zero voltage zero current switching is proposed [45] by utilizing the LC series compensation with an auxiliary network for achieving zero current switching (ZCS). This innovative topology employs a cost-effective controller to maintain a constant output voltage, even in the face of variable input voltage. It is designed to meet the highest standards of quality and reliability, making it an ideal choice for variable voltage applications. The author developed a 1.1KW prototype and tested it for efficiency and found it to be 91.26% with ZVZCS. Another author in [46] proposed a high-efficiency WPT system with one inverter and one active rectifier with phase-shift angle control aiming the objective of reducing EMI and increasing efficiency. Here optimum power angle range is also evaluated to control the power loss and achieve the transfer efficiency of 95.2% with a 500W prototype taking 0.2 as the coupling factor.

A hybrid WPT is proposed in [47] to work in charging pad misalignment conditions. This hybrid WPT achieves high misalignment tolerance with CC and CV mode inherently by connecting two coils in series reversed connection on the transmission side and two coils with series and series-parallel compensation respectively on the receiver side. Hence without adding any additional converter, the control complexity is reduced and increases system reliability with a maximum efficiency of 93.4% in a 1KW experimental prototype. In [48] a Dual-LCC compensated WPT system with SCC is implemented for EV charging supporting a wide output voltage regulation with improved overall efficiency. Triple-phase-shift (TPS) control strategy including a switch-controlled capacitor (SCC) is incorporated in the dual active bridge rectifier to obtain the specified characteristics

TABLE 6. Wireless charging topologies comparison.

Topology	Rating (W)	Freq (kHz)	Switches	Diodes	HF Transformer	Efficiency (%)
Full bridge Converter[44]	500	84.5	8	0	1	95.2
Buck-Boost Integrated Full Bridge[45]	500	84.5	4	4	1	94.9
Dual Active Bridge Converter[46]	1,100	85	4	4	2	91.26
Full bridge Converter[47]	1,000	85	8	0	1	92.5
Dual Active Bridge Converter[48]	1,000	85	4	8	2	93.4
Full bridge Converter[49]	400	200	4	4	1	90
Full bridge Converter[50]	3,000	85	4	4	1	91.4
Full bridge Converter[51]	618	85	4	4	1	95
Full bridge Converter[52]	250	85-90	4	8	1	89-91
Full bridge Converter[53]	700	85	5	5	1	85.2
Dual Active Bridge Converter[54]	3700-22000	40 & 85	8	0	1	-
Full bridge Converter[55]	4,000	20	4	4	1	96.3

with load matching and zero voltage switching. Maximum efficiency is obtained for the complete power range by adjusting the capacitance to the optimum value. Table 6. gives the summary of the topologies employed for wireless charging of BEV with the converter rating and peak efficiency along with the number of switches used in the converter.

C. HYBRID CHARGING

Hybrid Charging technology has the functionality of both plug-in and wireless charging technologies and has the combined advantages. Fig. 3 (c). gives the basic operational diagram of a hybrid charging method. The hybrid approach implemented in [56] for integrating plug-in and wireless charging capabilities with onboard boost converter integration is an optimal solution for electric vehicle users while maintaining essential isolation. The prime benefit of the integrated charger is that the EV charging current has less ripple. The hybrid system developed in [57] shares the power module for both modes of operation to lessen the cost and the reduction of the rated power module is achieved by an improved parameter evaluation technique for evaluating the coupling inductance of the WPT. In another work [58] taking the high-frequency transformer as the coupling point, a hybrid conductive and inductive charging system is developed aimed at the sharing of circuit components, thereby reducing the size and complexity. The drawback of the method is that the simultaneous operation of inductive and conductive modes is not achieved. In [59] an advanced dual-loop hybrid control strategy has been devised by combining and Sinusoidal Ripple Charging (SRC) and Constant Current - Constant Voltage (CC-CV) control methods to facilitate WPT and wired charging, respectively. The front-end MBMC is designed to ensure a steady DC voltage at the DC link, while simultaneously extracting a sinusoidal current input without phase change from the supply voltage. This approach enables the proposed charger to operate at an almost unity power factor (UPF). Another approach of integrating wired and wireless charging is introduced in [60] which drives multiple independent loads simultaneously with a non-isolated single inductor DC-AC buck-derived hybrid converter with multiple outputs. This method is implemented for low-power applications and is simple and cost-effective with high efficiency and increased power density. An adjustable turn-ratio method [61] for the transformer is applied in the integration of a wired/wireless charging system. The secondary side voltage reduction is applied by adjusting the transformer turn ratio depending on the DC-link voltage. A hybrid conductive/contactless EV charger with PV-grid integration is introduced in [62] to reduce the cost and losses in the hybrid charging system by sharing the high-frequency inverter for both conductive and inductive transfer modes. A novel method of integrating the WPT and OBC system of EV charging is given in [63] to reduce cost, complexity, and weight with high power density. A three-coil system is formed with OBC, WPT and receiver sides with integrated conductive/inductive modes of operation. In OBC operation mode a better coupling exists between the OBC and receiver coils thereby transporting power from the OBC to the battery system and eliminating the WPT mode. In the WPT operation mode, the relay on the OBC opens making the power transfer between WPT and receiver coil and hence charges the battery through wireless mode. Table 7. gives the summary of the topologies employed in the references for hybrid charging of BEV with the converter rating and peak efficiency.

D. INFERENCE

Among the various charging methods of EVs, the comparisons in Table 5, Table 6, and Table 7 wired charging offers the highest efficiency compared with the wireless method of charging. The efficiency in wired charging depends on

TABLE 7. Hybrid charging topologies comparison.

Topology	Rating (W)	Freq (kHz)	Switches	Diodes	HF Transformer	Efficiency (%)
Boost Integrated Hybrid Converter[56]	6,600	22	6	2	2	86.2
Half Bridge Buck-Boost Converter[57]	15,000	85	2	4	1	91.6
Full Bridge Converter[58]	3,000	CM 100 to 135 IM 85	8	4	1	CM 93 to 97.4 IM 87 to 93.6
Totem-Pole PFC Converter[59]	3,300	CM-50 IM-85	12	0	2	-
Buck Derived Hybrid Converter[60]	20	100	4n	3	-	88
Full Bridge Converter[61]	3,600	CM-300 IM-85	12	8	2	CM-77 to 82.2 IM-76.9 to78.7
Full Bridge Converter[62]	3,300	85	8	8	2	-
Full Bridge Converter[63]	1,200	85	12	-	1	-

CM-Conduction Mode, IM-Induction Mode

factors such as the count of switches employed, the converter switching frequency, converter design and topology and the Power conversion stages included. For the hybrid environment where slow and fast charging is simultaneously required, multi-port converters shall be preferred which reduces the use of active switches as one-third of the separate converters for slow and fast charging. In the event of low voltage applications such as in fuel cells, high-capacity switches are required, but they are very expensive and instead of preferring high-capacity switches paralleling of low-capacity switches can be done for handling the same current capacity considering the cost of switches. An increase in the number of switches and switching frequency increases the switching loss of the converter, hence the converter should be optimized for soft switching in loss minimization. The efficiency of the WPT in turn depends on the switching frequency and according to the WPT standard SAE J2954 the frequency range is limited to work between 81.9-90 kHz [92]. Hence for achieving high-efficiency WPT charging adhering to the standards we can prefer an SSWPT converter thereby switch count decreases and total switching loss also decreases.

III. SINGLE-STAGE TOPOLOGIES FOR WIRELESS CHARGING

In this section, the single-stage converters utilized for EV wireless charging are discussed [93], [94], [95], [96], [97], [98], [99], [100], [101], [102], [103], [104], [105], [106], [107]. The single-stage represents that the converter operates with two or more functionalities without additional converters. Apart from the regular converters, single-stage converters are preferred because of their simpler circuit model with fewer components and improved efficiency than the regular converters for wireless charging. The single-stage converters can be classified based on the input source AC or DC as (i) Single-stage Converter with DC Input and (ii) Single-stage Converters with AC Input. The AC input Single-Stage converters shall be further divided into (a) Single-Phase Single-Stage WPT Converters and (iii) Three-Phase Single-Stage WPT Converters which is represented in Fig. 4 with a chart.

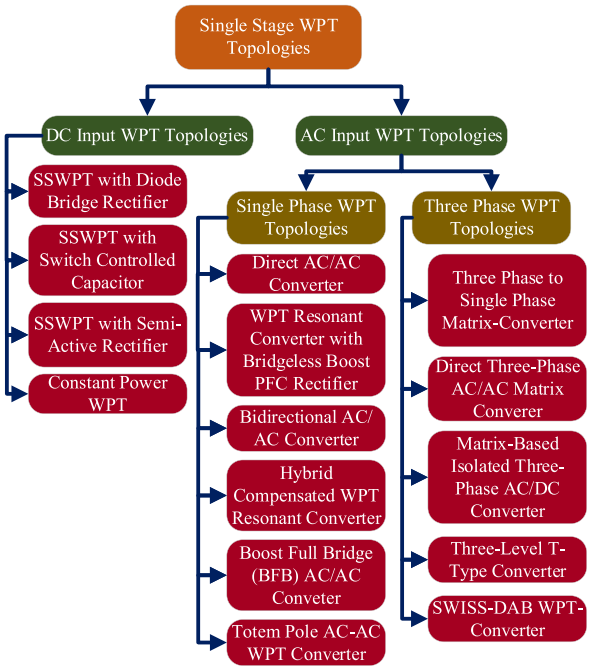

FIGURE 4. Classification of single-stage WPT topologies.

A. DC INPUT WPT TOPOLOGIES

The topologies with DC input proposed in works of literature [93], [94], [95], [96] were discussed here. The authors adopted the CC-CV charging process, where constant current (CC) charging is required initially for the discharged battery to charge up to the specified battery voltage and a constant voltage (CV) charging till the battery gets fully charged. Constant power (CP) charging is utilized to improve the efficiency during the charging process in the fixed frequency operation mode with the combined advantages of load-independent transfer characteristics and

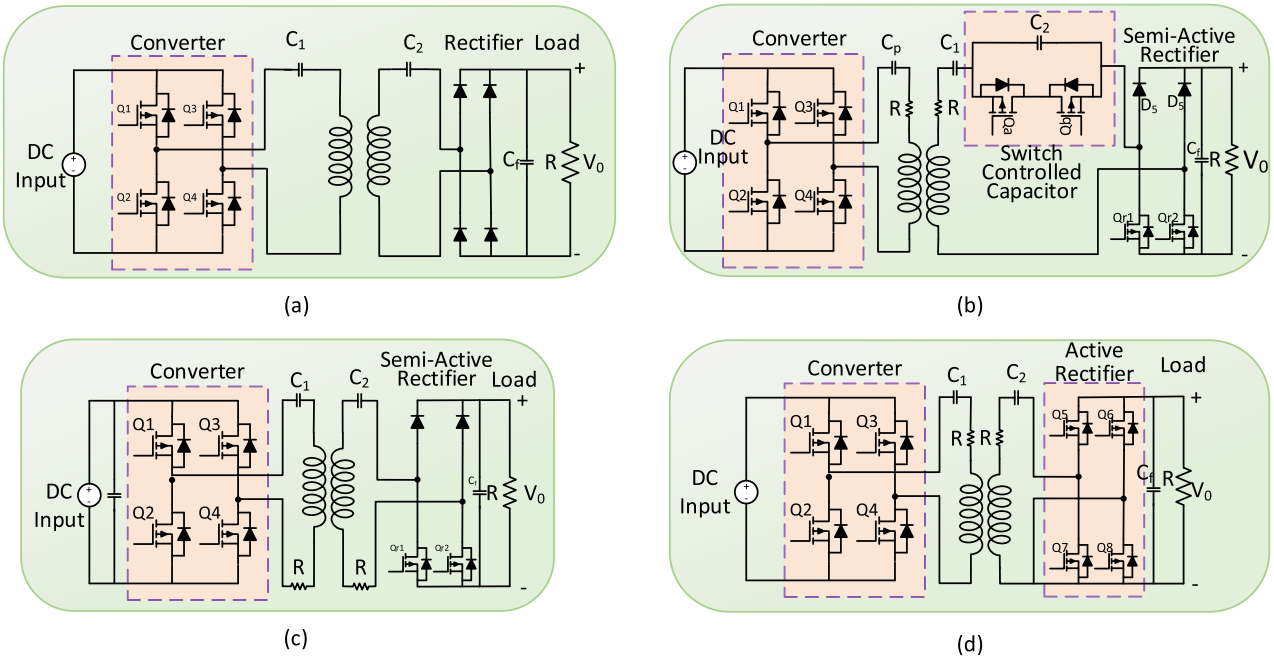

FIGURE 5. DC input single-stage WPT topologies (a) SSWPT with Diode Bridge Rectifier (b) SSWPT With Switch Controlled Capacitor (c) SSWPT with Semi-Active Rectifier (d) Constant Power WPT.

load impedance equalizing methods. The constant operating frequency reduces the requirement for wireless feedback communication and an additional DC-DC converter is not necessary for voltage control, as the receiver side achieves a CC/CV charging profile with output regulation. The CC/CV charging process and optimal efficiency achievement were both implemented in the SSWPT converter. For maximizing efficiency and reducing losses, constant power charging is adopted. A novel control strategy is developed by optimizing ZVS, minimum reactive power and minimum overall loss conditions, to yield CP output and maximum efficiency.

1) SSWPT WITH DIODE BRIDGE RECTIFIER

The SSWPT offer high efficiency and an easy control mechanism. Fig. 5 (a) gives the circuit diagram for SSWPT with a diode bridge rectifier. In work [93], the SSWPT operating at Load load-independent current mode achieves the constant current charging profile and operating at Load load-independent voltage mode achieves the constant voltage profile for the battery. In LIC mode achieves the easy control mode and high efficiency of operation and in LIV mode the control losses in the converter are eliminated. Though the ZVS is employed the Turn-On switching loss is still present in the circuit during the control. Because of reasons like not considering the switch-off losses, non-linearity of the output diode bridge rectifier, not considering the harmonic components and not considering the diode's forward voltage the practical efficiency achieved is lesser than the theoretical findings. The variation of efficiency and load quality factor is plotted and it indicates that the high efficiency is obtained in higher quality factor in CC mode than in CV mode. The converter working in LIC mode could not achieve Constant Voltage charging as the control range is very narrow and is suitable for achieving soft switching operation with load variation.

2) SSWPT WITH SWITCH CONTROLLED CAPACITOR

Due to the drawback that the load range is wide and maximum efficiency cannot be maintained throughout the load range during charging, the Constant Power charging method [94] is employed in the SSWPT, where the secondary side control is adopted with Semi-Active Rectifier and SCC for the combined advantage of load impedance transfer characteristics and load matching. Fig. 5 (b) shows the circuit representation for SSWPT with a switch-controlled capacitor in which Wireless feedback communication is not required as the converter operates in Fixed operation frequency control mode and with secondary side real-time regulation. With the experimental results, it is noticed that the variation in conduction angle directly affects the output power and hence the control angle of SCC is varied in accordance with the conduction angle. The drawback of the CP charging method is that at a very low value of k (serious misalignment), to maintain CP a large input current is required resulting in circuit damage and hence protection is needed for the circuit.

3) SSWPT WITH SEMI-ACTIVE RECTIFIER

An SSWPT with Phase Shift PWM applied at the transmitter side in work [95], provides wide load range efficiency with the benefits of CC and CV modes of charging and is shown in

TABLE 8. DC input single stage WPT topologies comparison.

Ref.	Topology	Power (Watts)	Switching Frequency (kHz)	Input Voltage (V)	Output Voltage DC (V)	Switch Count	Diode Count	Inductor Count	Capacitor Count	Total Count	Cost ($)	Weight/ Size	Efficiency (%)
[93]	SSWPT with Diode Bridge Rectifier	1500	50-68.5	190	175	4	4	0	3	11	229	*	96
[94]	SSWPT With Switch Controlled Capacitor	150	85	48	51-84.6	8	2	0	4	14	325	**	88
[95]	SSWPT with Semi-Active Rectifier	1000	50	155.5	170	6	2	0	4	12	743	**	94.35
[96]	Constant Power SSWPT	120	50	80	55-78	8	0	0	3	11	347	*	87.5

S=Switch, D=Diode, I=Inductor, C=Capacitor, *Light /Small, **Moderate/Medium, ***Heavy/Large

Fig. 5 (c). The constant frequency operation in the transmitter reduces the requirement for wireless feedback communication. The SAR in the battery side regulates the output, thereby additional DC/DC converter is not needed in the battery side. During the CC approach, the receiver side acts as a passive rectifier and during CV mode the voltage feedback is provided to SAR to achieve the load-independent output voltage. During the battery charging process, the desired output and efficiency are obtained by varying the conduction angle on the transmitter side and the phase-shift angle on the receiver side of the SSWPT. A faster response of the controller is achieved in the rectifier side than that of the inverter side because of the dependability of the inverter conduction angle on the conduction angle of the rectifier.

4) CONSTANT POWER WPT

The drawbacks such as frequency modulation, instability and circulating reactive power in the conventional WPT can be overcome by single-stage CP WPT [96]. The CP-CV charging is superior to the CC-CV method in implementing the fast-charging WPT. The circuit for constant power WPT is given in Fig. 5 (d). An optimized efficiency strategy is achieved by perturbation and observation method which minimizes the power loss in the input converter, active rectifier and magnetic coupler. By utilizing the equivalent magnetic coupler, optimal efficiency can be achieved through impedance matching. During the charging process, the system can accomplish ZVS, low circulating power and reduced total losses by proper control action of conduction angles in the transmission side inverter, receiving-side controlled rectifier, and phase shift between either side. On examining experimental studies, it is observed that the ZVS condition is simultaneously achieved with a low value of circulating KVAR.

5) INFERENCE

Table 8 gives the comparison of single-stage DC/DC converter topologies with the CC, CV, CP and ZVS modes of operation and the control strategy implemented. In the referred methods ZVS method is employed to reduce the switching losses with constant frequency operation. The WPT circuit representation for the DC input topologies is given in Fig. 5. Comparing all the methods the efficiency of the converter depends on the number of switches involved in the converter circuit. Being 4 switches and 4 diodes used in the literature [93] gives a peak efficiency of about 96% without considering losses in the diodes and being 8 switches used in the literature [96] results in an efficiency of about 87.5%. Hence by reducing the stages of conversion and switch count the efficiency of the WPT scheme can be increased to a considerable extent. The absence of the rectification process in the front stage makes the DC input topologies a simpler circuit which contributes to loss reduction.

B. AC INPUT WPT TOPOLOGIES

Since the main source of supply is the AC supply the AC input WPT topologies are referred for EV charging applications. The extensively used converters in Single-stage Wireless Power Transmission are the matrix converters converting the grid frequency AC into AC with suitable increased frequency at the required amplitude. To reduce the stress on converter switches, power loss, and electromagnetic interference (EMI), the ZCS method is adopted in the direct AC-AC converter. If there exists an Equivalent Series Resistor (ESR) or any coupled load in the circuit, always power is consumed by the circuit. The SiC MOSFETs offer greater cooling and reduced power losses with increased power density, preferred in many suitable applications. High-speed SiC MOSFET is the best option for the production of high-frequency waveforms through a single-stage power conversion. To regulate the output power, resonant current and voltage, a variable-frequency controller strategy is implemented in the SSWPT Converters. An energy-injection process and free-oscillation method-based SSWPT design provide high efficiency with low electromagnetic interference. The energy injected decides the resonant current amplitude of the LC

tank circuit. In the digital simulation studies, the total harmonic distortion (THD) in the grid current is found to contain a value of 19%. This distortion is mainly attributed to their control strategy. To achieve more flux distribution, the inter-turn space should be kept minimum in the single-stage grid integrated topology, which results in UPF. Single-stage WPT resonant converter with a multi-compensation design better suited for medium and high-power wireless charging requirements. The boost full bridge (BFB) AC-AC converter adopting an asymmetric modulation scheme in the primary converter gives better controllability to achieve PFC and output regulation. A hybrid LCC series-parallel (LCC-SP) compensation network is used in SSWPT to realize CCO and CVO. The AC input single-stage WPT topologies are further divided into single-phase single-stage WPT (SPSSWPT) and three-phase single-stage WPT (TPSSWPT) topologies.

C. SINGLE-PHASE SINGLE-STAGE WPT TOPOLOGIES

The Single-phase Single-stage topologies [97], [98], [99], [100], [101], [102] employed for WPT are discussed here. The single-phase topologies are the most widely utilized form of conversion since the utility grid consists of the AC supply which should be transformed to high-frequency AC and transmitted wirelessly then rectified into DC for the EV. The large DC link capacitor is not required in the event of single-stage converter implementation. The SSWPT bridgeless boost PFC rectifiers will have reduced conduction loss due to fewer switches present in the converter. The circuit topologies are shown in Fig. 6 for various literature on SPSSWPT.

1) DIRECT AC/AC CONVERTER

A simple design with four switches constitutes the direct AC/AC converter [97] that has the capability of producing high-frequency AC for the WPT system. In Fig. 6 (a) the circuit of the direct AC/AC converter is shown. The energy injection principle to the load is applied whenever necessary, which requires a simplified controller design. This direct converter efficiently generates an AC output of the required frequency for seamless contactless power transfer, with the added benefit of reduced switching and zero reverse power flow. ZCS operation can be realized for the direct AC/AC converter and the presence of equivalent series resistors (ESRs) always consumes some power. Based upon the theoretical and practical analysis this topology offers full control on maintaining current quality with reduced EMI. Since the Q factor of the designed system is high it offers very low damping current control. Even though the ripple content in the current is too low. The advantage of this topology is that it has better steady-state and dynamic responses. The drawback of current overshoot and current ripple arises in the cases of over-injected energy and overconsumption of the load respectively.

2) BRIDGELESS BOOST PFC WPT RESONANT CONVERTER

WPT system faces many drawbacks in achieving high power, efficiency and power factor in EV charging applications. Improving the same needs two or more conversion stages in the conventional system, which reduces the efficiency of the system. A WPT converter with a PFC rectifier given in Fig. 6 (b) is proposed by [98] to improve converter efficiency and quality of power with the added benefit of reduced costs and minimum complexity for WPT in high-power applications. Bridgeless PFC rectifiers have lower conduction loss with fewer semiconductor devices. In the front end, the conversion stages of PFC, rectifier and high-frequency inverter were achieved by the SSWPT resonant converter added with boost PFC rectifier. The experimental results reveal that the presence of harmonic varies from 22 to 15% in the entire load range with an achievable power factor of more than 97%. The efficiency of the proposed converter ranges from 81% to 90% for load variations of 20% load and full load respectively.

3) BIDIRECTIONAL AC/AC CONVERTER

For better Reliability and a simple control strategy, a single-stage Bidirectional AC/AC Converter given in Fig. 6 (c) from [99] is implemented for the WPT system. The UPF feature is achieved with an acceptable G2V and V2G efficiency as per the SAE guidelines, although provided weak communication link, smaller bandwidth sensors and reduced component count with the single controller but the control strategy implemented results in higher grid current harmonics and likely to have ripple component with twin frequencies in the battery current. A validation analysis is carried practically for G2V and V2G modes of bidirectional operation for the proposed converter and observed to obtain a very good power factor of 0.99 in either mode and with the presence of harmonic content of 11.7 % in G2V and 12.62% in V2G modes. The transient analysis reveals the controller has a good dynamic response for the proposed method with UPF operation.

4) HYBRID COMPENSATED WPT RESONANT CONVERTER

The bridgeless PFC boost rectifier implemented for WPT has the problems of DC-link voltage rise and unstable converter output voltage which makes the CCO and CVO analysis difficult. Hence an asymmetric modulation method is applied with hybrid compensation to overcome the above problems and obtain the load-independent output. The Hybrid Compensated WPT resonant converter [100] achieves the combined operation of the rectification, PFC, and dc/dc conversion in a single stage with increased power density. Fig. 6 (d) depicts the circuit diagram for a hybrid compensated WPT resonant converter. Experimental studies show that the power factor is above 0.99 for both CC and CV approaches in the developed system with input side THD less than 18% and at full load it settles to a value of 11%. The losses are somewhat higher when compared to non-PFC systems but with improved input power quality.

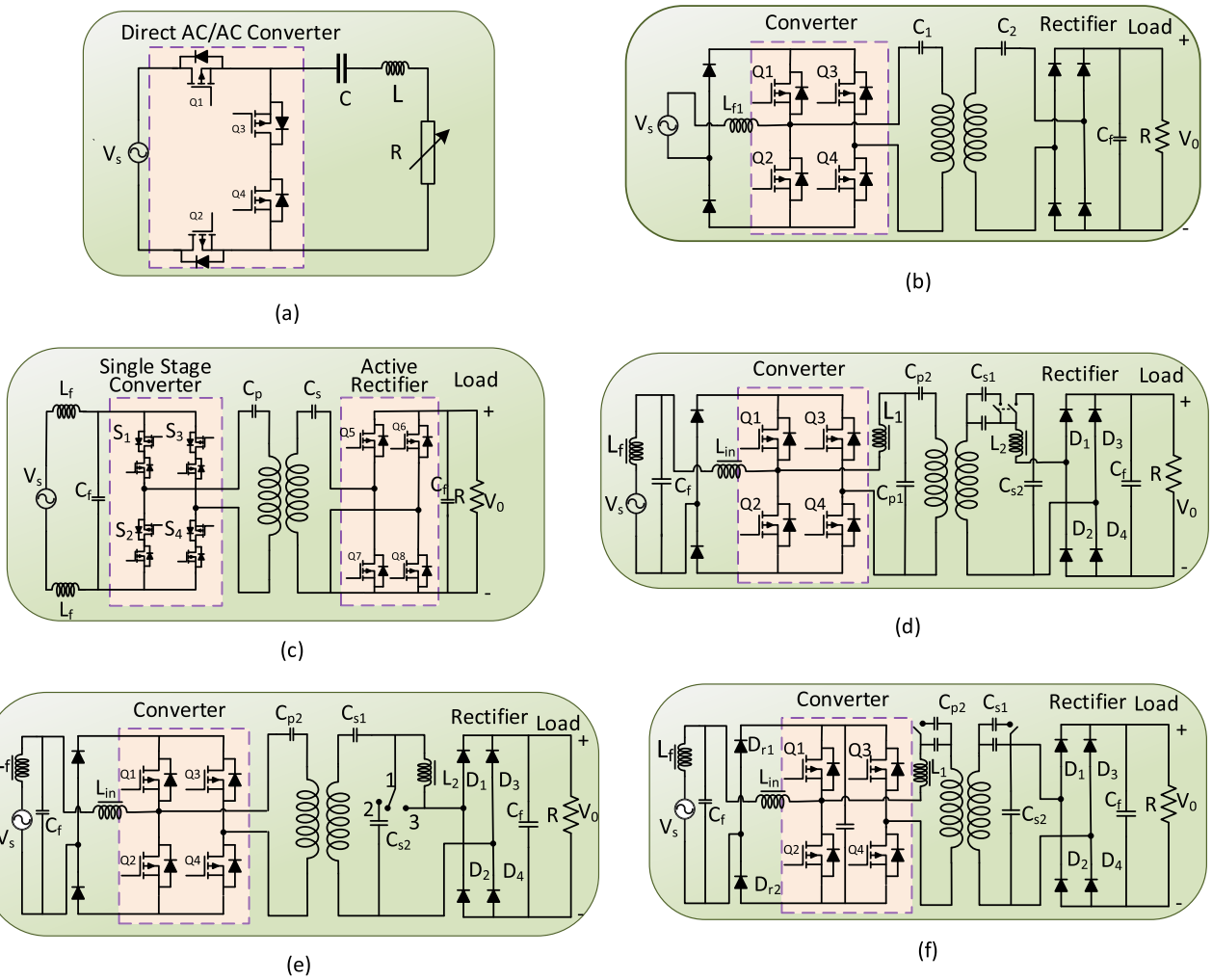

FIGURE 6. Single-Phase Single-Stage WPT Topologies (a) Direct AC/AC converter (b) Bridgeless boost PFC WPT resonant converter (c) Bidirectional AC/AC Converter (d) Hybrid Compensated WPT resonant converter (e) Boost Full-Bridge AC/AC Converter (f) Totem Pole AC/AC WPT converter.

5) BOOST FULL-BRIDGE AC/AC CONVERTER

Boost Full-Bridge AC/AC converter is a bridgeless totem pole rectifier integrated with the full-bridge type inverter [101]. An asymmetric modulation method is introduced in the BFB AC/AC converter for achieving PFC and output regulation simultaneously by duty cycle control of each switch in the primary converter. This asymmetric modulation scheme with duty-cycle adjustment can maintain constant DC bus voltage and reduce voltage stress on primary converter devices during light load. Combined hybrid compensation and asymmetric modulation schemes provide the CC and CV output. The circuit illustration for the boost full bridge AC/AC circuit is shown in Fig. 6 (e). The variable switching frequency operation in critical conduction mode (CRM) of the totem-pole bridgeless rectifier makes it difficult in integrating to the full-bridge inverter. In continuous conduction mode, the control complexity increases and the soft switching operation becomes difficult. From a quality perspective, this topology offers a better power factor value of 0.993 in CC mode which is less than in CV mode with the highest possible efficiency of 88.17% considered to be comparatively low for this SPSSWPT system. The transient study reveals that the switching between SS and S-LCC compensation modes does not affect the load too much.

6) TOTEM POLE AC/AC WPT CONVERTER

The Totem Pole AC/AC WPT Converter exhibits the drawback of control complexity in implementing ZVS while realizing CCO and CVO. To overcome the drawback a series-parallel LCC combination (LCC-SP) is introduced for SSWPT [102] compensation and the circuit model is represented in Fig. 6 (f). The primary coil current remains unchanged in both CC and CV operational modes and also, the transfer ratios in both modes are not restricted by the values of LCT. The LCC-SP compensation network has a single high-frequency resonant inductor, which reduces the circuit cost. According to the findings of the experiment, it was noted that the ZVS condition is attained by modifying the input

TABLE 9. Comparison of single-phase single-stage WPT converter topologies.

Ref.	Topology	Power (Watts)	Switching Frequency (kHz)	Input Voltage (V)	Output Voltage DC (V)	Components Count	Total Count	Component Cost ($)	Weight/ Size	Efficiency (%)	THD (%)	Power Factor
[97]	Direct AC/AC converter	10	30	20	-	4S 0D 1I 1C	6	84	*	-	-	-
[98]	Bridgeless boost PFC WPT resonant converter	2560	110	220	320	4S 6D 1I 4C	5	1649	**	90.1	15.4	0.99
[99]	Bidirectional AC/AC Converter	3700	85	-	-	8S 0D 2I 2C	12	735	**	89.2 G2V 88.8 V2G	11.7 G2V 12.62 V2G	0.99 G2V 0.99 V2G
[100]	Hybrid Compensated WPT resonant converter	360	85	110	72	4S 6D 4I 8C	22	722	***	90.06	11.1	0.994
[101]	Boost Full-Bridge AC/AC Converter	720	100	110	144	4S 4D 3I 6C	17	510	***	88.17	-	0.993
[102]	Totem Pole AC/AC WPT Converter	360	85	110	72	4S 6D 4I 9C	23	791	***	90.15	High	-

S=Switch, D=Diode, I=Inductor, C=Capacitor, *Light /Small, **Moderate/Medium, ***Heavy/Large

impedance angle, which facilitates a seamless shift between Continuous Conduction Mode (CCO) and Continuous Voltage Mode (CVO). The highest transmission efficiency of the SSWPT system is achieved in the test system and the LCC-SP compensation system is dependable and cost-effective. In the aspect of reducing switches, some passive components need to be added to improve efficiency. The higher-order harmonics need to be eliminated for the implemented asymmetric control method by introducing the LCC-SP circuit which makes the converter less harmonic.

7) INFERENCE

The circuit implementations of the single-phase AC topologies are given in Fig. 6. The comparison of converter topologies employed in single-stage is presented in Table 9. Almost all the articles in single-stage single-phase converters consist of 4 switches considered to be the minimum number of switches with an achieved peak efficiency between 88-91%. Though only a minimum number of switches were used, the peak efficiency is found to be still less than 91%, and the harmonic content in the SPSSWPT literature is quite above 10% and some literature does not focus on the power quality point of view which shows there is a need for further improvement in the single-stage topologies where there is a wide gap in attaining a better power quality.

D. THREE-PHASE SINGLE-STAGE WPT TOPOLOGIES

For high power capacity, highly efficient power transfer, and high power quality applications the three-phase single-stage WPT topologies [103], [104], [105], [106], [107] with galvanic isolation are preferred. Without increasing the number of stages, the PFC and bus voltage control methods are achieved in the TPSSWPT resonant converter by implementing a T-type topology in the circuit, thereby minimizing the circuit complexity and price of the WPT system. The TPSSWPT converter topologies employed for reducing switching loss and the size of the converter are given in Fig. 7.

1) THREE-PHASE TO SINGLE-PHASE-MATRIX-CONVERTER

An AC/AC converter with matrix converter topology [103] with minimum switches is implemented, which converts a 3-phase utility system voltage to a high-frequency voltage suitable for a series compensation-based WPT system. The circuit diagram is given in Fig. 7 (a). Efficient high-speed SiC MOSFETs were utilized in the matrix converter for generating high frequency current and single-stage conversion achieves efficiency improvement with power loss. Out of the two four-step commutation methods for matrix converter, four-step voltage commutation is preferred because of the difficulty in tracking the sign of the high-frequency load current. A modulation scheme of varying phase shifts is applied to the WPT converter. The overall efficiency achieved by the matrix-type converter is less due to the input filter, compensating capacitor, wire connections and internal power source. The problem of large phase shifts results in high power loss, which can be reduced by adopting the proposed converter. The results of the developed converter with a 300W rating achieve the near UPF with low grid side THD.

2) DIRECT THREE-PHASE AC/AC MATRIX-CONVERTER

Efficiency improvement is the major concern in developing a direct 3-phase AC/AC matrix converter [104] with soft switching operation, that also performs a reduction of stress and losses in the switches employed, with minimum

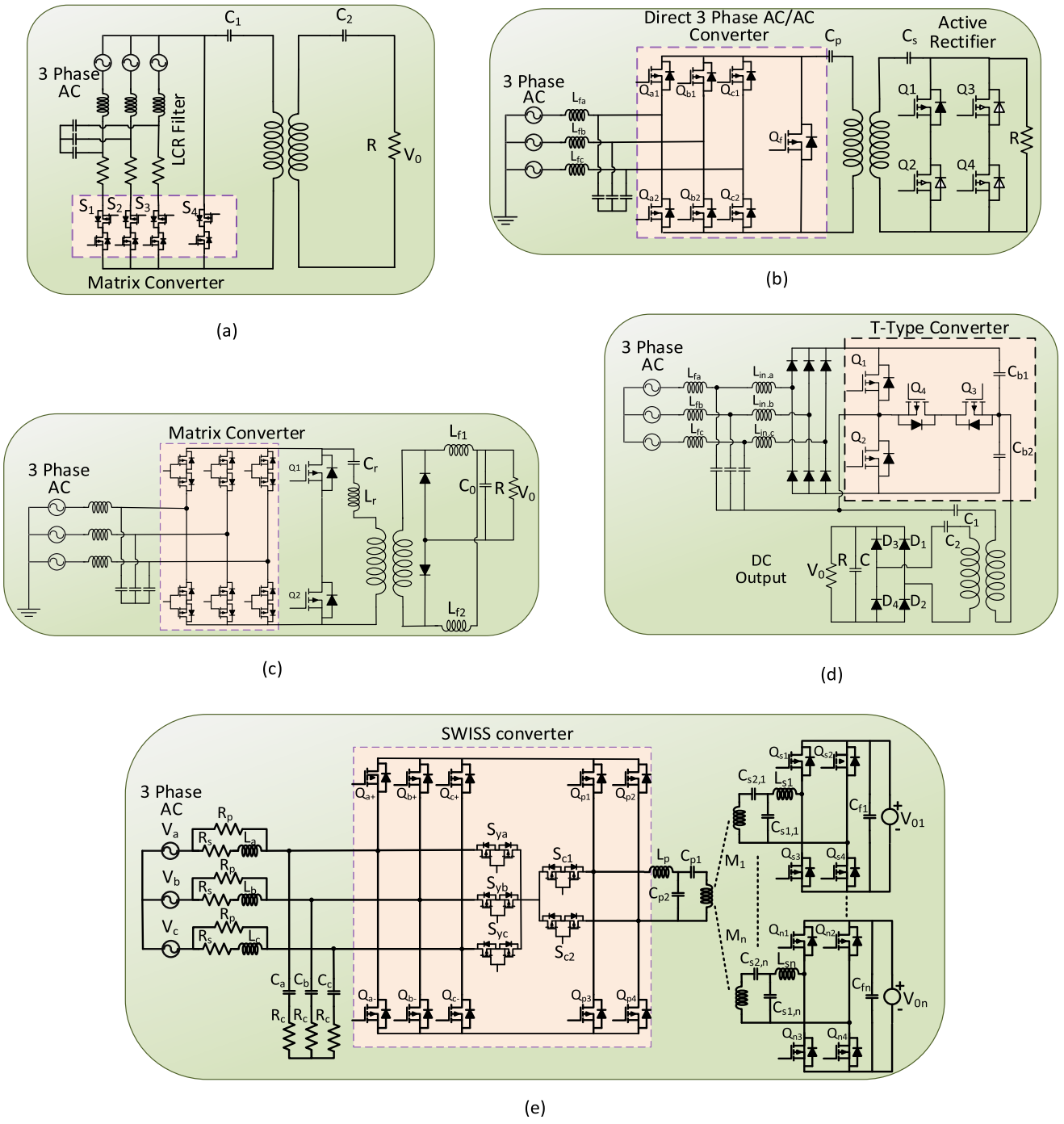

FIGURE 7. Three-Phase Single-Stage WPT Topologies (a) Three-Phase to Single-Phase-Matrix-converter (b) Direct Three-phase AC/AC Matrix-converter (c) Isolated three-phase AC/DC matrix-converter (d) Three-level T-type Converter (e) SWISS-DAB IPT-converter.

EMI problem. This matrix converter topology is shown in Fig. 7 (b). An energy-injection and free-oscillation method-based SSWPT design provides high efficiency with low electromagnetic interference. During resonant current regulation control, the energy fed to the LC tank circuit must be taken into consideration as it directly affects the current amplitude and can be accomplished by continuously altering the converter's operation mode from energy-injection modes, and vice versa. The current control methodology incorporated in the system makes the dynamic adaptability of the converter for the required reference setting. The results of the proposed topology indicate a better converter efficiency of about 88.2% with a low value of current THD of 14.3% which differs slightly from the calculated values. The power factor

TABLE 10. Comparison of three-phase single-stage WPT converter topologies.

Ref.	Topology	Power (Watts)	Switching Frequency (kHz)	Input Voltage (V)	Output Voltage DC (V)	Components Count	Total Count	Component Cost ($)	Weight/ Size	Efficiency (%)	THD (%)	Power Factor
[103]	Three-Phase to Single-Phase-Matrix-converter	300	50	50	-	4S 0D 3I 5C	12	418	**	85	low	Almost Unity
[104]	Direct Three-phase AC/AC Matrix-converter	267	12.25	40	-	7S 0D 1I 1C	9	100	*	88.2	14.3	0.67
[105]	Isolated three-phase AC/DC matrix-converter	500	40	115	48	8S 2D 6I 5C	21	433	***	88.64	3.06-5.8	Almost Unity
[106]	Three-level T-type Converter	3300	85-90.5	220	330	4S 10D 6I 3C	23	445	***	89.2	3.5	Unity
[107]	SWISS-DAB WPT-converter	1200	40	220	120-380	20S 0D 4I 5C	29	722	***	95.2 G2V 91.2 V2G	2.5	0.993

S=Switch, D=Diode, I=Inductor, C=Capacitor, *Light /Small, **Moderate/Medium, ***Heavy/Large

is considerably less because of the existence of harmonics in the grid side voltage and current.

3) ISOLATED 3-PHASE AC/DC MATRIX-CONVERTER.

The matrix converter has the property of converting fixed AC to variable AC with reduced energy storage capacitors and is hence implemented for converting low-frequency AC to high-frequency AC for WPT applications. Utilizing the matrix topology an isolated 3-phase AC/DC matrix converter [105] is implemented for EV charging applications. In the circuit given in Fig. 7 (c) two of the switches involve Natural ZVS and in turn switching losses get reduced in the converter. The two switches turn on with dead time and this does not impact the efficiency of the power converter. By implementing a CDR circuit in the WPT, the turn ratio of the transformer is lowered, thereby effectively decreasing the shunt inductance of the HFT. The SVM PWM method enhances the input power quality of the WPT converter. For high power density applications, the single-stage converter with galvanic isolation is suitable and also it can be utilized for high conversion efficiency, and input PFC-demanding applications. A 500W test system is developed, which provides the results of efficiency and THD as 87.5% and 5.8%. and the deviation from theoretical calculations is due to the ignorance of ripple and ESR in the evaluation of losses. In order to get the desired fast response a fast-acting controller must be utilized.

4) THREE-LEVEL T-TYPE CONVERTER

The high number of switches and passive components in WPT introduces control complexity and reduces efficiency, hence the approach for T-type Topology [106], which functions for both the PFC and DC-DC WPT operations concurrently.

The Fig. 7 (d) shows the T-type circuit topology implemented. As the conventional frequency control method could not achieve the PFC and bus voltage control, a new method with three-level voltage and duty ratio adjustment is adopted for the WPT converter. ZVS operation could be implemented in the proposed converter only when the load value is greater than half load. With the experimental results, it is evident that the maximum overall efficiency attained is 89.2% with an input THD value of 3.5% at the unity power factor. Regarding power loss among the total half of the total losses are due to the input inductor which requires an efficient design with a small permeance value. Moreover, in the three-phase single-stage topology the absence of the zero sequence components provides a better input power quality.

5) SWISS-DAB WPT-CONVERTER

The challenging feature of getting a sinusoidal input current is achieved by SWISS-DAB WPT-converter [107] in which the other features such as ZVS, and high efficiency were also achieved. In Fig. 7 (e) the two-sided LCC compensation system enhances transfer efficiency and the simple PI control strategy is utilized for the converter control. The losses in the inverter bridge and the pickup side rectifier bridge are low due to the ZVS operation but higher when compared to the primary side three-phase rectifier bridge. The bidirectional converter designed in this literature provides an experimental efficiency of 95.2% during V2G operation and 91.2% during G2V operation. The power factor achieved at 1.2KW is 0.993 with a harmonic content of 2.5% on the input side. The overall performance achieved is much better than the conventional topologies other than the increase in components count. A more precise value of current feedback is required for further improvement of power factor and THD values.

TABLE 11. Advantages and disadvantages of single-stage WPT converter topologies.

Type	Topology	Advantages	Disadvantages
DC input WPT Topologies	SSIPT with Diode Bridge Rectifier	• Optimal efficiency is achieved for the entire charging profile during CC and CV. • Soft switching is achievable for the entire battery load range. • Less control is required for LIC and LIV operations during CC and CV.	• Switching losses due to the transistor parasitic capacitor are ignored. • Efficiency decreases with an increase in μ. Where $\mu = \frac{Primary\ Resonant\ Frequency\ (\omega_p)}{Secondary\ Resonant\ Frequency\ (\omega_s)}$. • Existence of switching losses during the turn-off period. • Considers only fundamental frequency components for analysis.
	SSIPT With Switch Controlled Capacitor	• The charging rate is very fast. • Maximum efficiency is achieved throughout the charging process. • Load independent transfer characteristics. • Eliminates wireless feedback communication. • Low voltage stress.	• Component losses are ignored. • Primary side overcurrent circuit protection is needed in case of serious misalignment.
	SSIPT with Semi-Active Rectifier	• Simple hardware design due to constant frequency operation. • Wireless feedback communication is not required. • Increases stability during charging. • Maximum efficiency during charging is maintained over a wide load range. • Soft switching is realized in both the inverter and rectifier sides. • Misalignment tolerant and achieves high efficiency. • Receiver-side power regulation is achieved easily. • Minimized hardware cost.	• Increased cost. • Lack of load-matching ability in frequency hopping schemes. • Hard switching and increased power loss in dual-sided active switch schemes. • Need for wireless feedback communication in frequency modulation schemes.
	Constant Power SSIPT	• Free from thermal problems. • Increases battery life cycle. • Cost saving. • Alleviates stability problems.	• Turn-off losses and stress on power devices are more during the more negative primary currents. • Hard turn-off and conduction losses of MOSFET appear in the inverter and active rectifier. • Reverse recovery loss is not optimized.
Single-Phase AC Input WPT Topologies	Direct AC/AC converter	• Does not require a separate DC Link. • Natural circuit oscillation is sufficient for creating high-frequency resonance. • Reduces EMI, switching stress, and losses in the power switches. • Better steady state and dynamic responses.	• Track current consists of a small ripple current. • More energy is needed for maintaining constant track current under transient conditions.
	WPT resonant converter with bridgeless boost PFC rectifier	• Improved Efficiency with good power quality. • Reduces complexity and converter cost. • Both fundamental and higher-order components are included for analysis. • Increased system stability.	• Increased operating frequency of 110kHz. • Lower power density.
	Bidirectional AC/AC Converter	• Simple control strategy. • Increased reliability. • UPF operation. • Eliminates Higher bandwidth sensors and strong communication requirements.	• Increased reliability. • Decreased cost. • Higher Total Harmonic Distortion. • Spatial flux decreases with increased interspacing. • Ripple component existence requires additional filter requirements.
	Hybrid Compensated WPT resonant converter	• Maintains constant output voltage and DC link voltage. • High efficiency and less converter cost. • Transmission gain is independent of transformer design.	• Conventional control method is not applicable. • A larger input phase angle is required for ZVS operation. • Obtaining load-independent characteristics becomes difficult.
	Boost Full Bridge (BFB) AC/AC Converter	• Reduced cost, complexity and volume of primary converter. • Both ZVS and PFC can be achieved.	• Equivalent series resistances of compensator are ignored. • Boost ratio is small in PFC mode.

TABLE 11. *(Continued.)* **Advantages and disadvantages of single-stage WPT converter topologies.**

		• Reduced voltage stress under light load.	• Accurate design of DC bus capacitance is required because of ripples. • Optimisation is needed for circuit parameters and control methods.
	Totem Pole AC–AC WPT Converter	• Less impact due to Mode switching on the circuit. • Transformer parameters do not affect the transfer gain. • Low cost and high efficiency. • Smooth transition between the CC and CV modes. • Suppresses higher-order harmonics.	• Coupling variations affect the primary circuit and hence protection is needed.
Three-Phase AC Input WPT Topologies	Three Phase to Single Phase Matrix-converter	• Minimized power loss. • Low switch count. • Better commutation is achieved.	• More converter losses at low power operation. • Increase in phase angle and coupling coefficient reduces efficiency.
	Direct Three-phase AC/AC Matrix converter	• Increased life and high reliability. • Reduced Switching loss and EMI. • Functions better in dynamic conditions. • Electrolytic capacitors are not required.	• Current sags arise at the zero voltage crossings. • Reduced power factor in current regulation mode. • Fast-acting processors required. • Less efficiency and higher THD.
	Matrix-based isolated three-phase AC/DC converter	• Compact size and reduced weight. • Better input power quality. • Improved THD, and reduced switching loss. • Reduced copper loss due to the current doubler rectifier.	• A snubber circuit is required due to leakage inductance of HFT. • Poor power factor at low power output. • Limitations in filter capacitor value due to displacement power factor. • Requires extra switch for circulating the leakage energy of HFT.
	Three-level T-type Converter	• Improved efficiency and quality power. • Reduced cost and complexity. • No zero sequence components.	• Bus voltage imbalance occurs at a 180-degree phase shift. • Continuous tuning of phase shift is required. • Power loss in switches at half load is more than at full load.
	SWISS-DAB IPT-converter	• Improved efficiency and input current quality. • Provides protection during short circuits. • Eliminates DC link capacitance.	• More switches count. • Input current quality is affected at low load conditions.

6) INFERENCE

The comparison of TPSSWPT topologies is presented in the table 10. The TPSSWPT is mainly preferred in the case of high-power BEV charging requirements and efficiency comparison with the SPSSWPT was found to be considerably less. This represents the reduction in efficiency as the converter capacity increases, so careful design with optimized parameters maximizes the efficiency of the high-power converters. Also, the THD reduces to a great extent in the case of the TPSSWPT compared with the SPSSWPT due to the inherent capability of the third harmonic elimination.

SUMMARY

From the survey of the literature, the converter topologies employed in single-stage provide high efficiency as the number of switches gets reduced in the event of reducing power conversion stages in comparison to the traditional WPT converters. To achieve high efficiency, the converter should be maintained at the ZVS operating point. Table 11 gives the advantages and drawbacks of the single-stage topologies discussed in this section. Also, in Table 12 various parameters of the converters are compared. The comparison of the converters proposed with respect cost of the components utilized shows a uniform variation with respect to the converter rating and type of semiconductor preferred for specific applications. The literature concerning economy was implemented with minimum cost breaking the dependability on rating and cost. From the comparison of different topologies SPSSWPT is preferred for high efficiency requirements compromising the power quality and where quality is of major concern the TPSSWPT is preferred. Further, the power quality should be considered as it gets degraded and thus the converter should be maintained at the optimized operating point for multi-objective converter function. The power factor thus very much needed to be kept near unity by incorporating specific control techniques in the SSWPT, which was discussed in the next chapter.

TABLE 12. Comparison of DC-DC, Single-Phase and Three-Phase WPT converter topologies.

Parameter	DC-Input WPT	Single-Phase Single-Stage WPT	Three-Phase Singe-Stage WPT
Power handling level	Very High	Low	High
Weight	Light	Light	Heavy
Zero sequence component of current	-	Present	Eliminated
Stability	High	Comparatively Low	High
Harmonics	-	More	Less
Control circuit	Simple	Simple	Complex
Input Power Quality	-	low	Good
Switching Frequency	Less	More	Less
Reliability	Less	Less	More
Switching Losses	Less	More	Less
Voltage stress	Less	Less	High

IV. PF CONTROL TECHNIQUES IN WPT

Power factor improvement in WPT is one of the important features, where the input power quality is to be maintained without degradation near the unity value. The power factor control techniques [52], [99], [108], [109], [110], [111], [112], [113], [114], [115] employed for single-stage WPT converters were reviewed to find improvements in the power quality. Poor power factor systems have reduced energy efficiency and power transfer capacity due to the distorted current and conduction losses in the converters and contains harmonic content of higher order leading to the problem of Electromagnetic interference [108]. The boost circuit suffers from input grid current harmonics [99] due to the discontinuous conduction mode and reduces the power quality. The difference in phase angle between V and I results in power loss, an increase in circulating current and KVAR [110]. Thus, the PFC capability is of important concern in the design of WPT converters suitable for high-power applications.

1) RESONANT CONTROL TECHNIQUE

In the paper [108] the author proposed a valuable feature in the converter by implementing a single switching action for one cycle in the converter switches to achieve an input power factor very near to unity. By utilizing a resonant technique given in Fig. 8, it is possible to make the input current into a sinusoidal waveform that can be made to track the high-frequency sinusoidal source voltage, thereby achieving a unity power factor. The experimental results of this literature show that the phase comparison control employed for the AC-DC power converter yields better power factor at different power levels. The THD values of this simple control vary between 14-23 % at the specified power level and it indicates that it has to be further reduced to a minimum value. The overall efficiency obtained is comparatively less than all of the discussed methods here. Hence in achieving better power quality the other key factors such as efficiency, and THD, lie in a reasonable range which needs to be improved further.

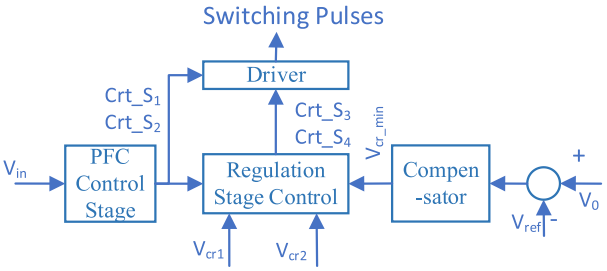

FIGURE 8. Phase comparison for AC-DC power converter.

2) H-BRIDGE SWITCHING PWM CONTROL

The inherent property of power factor correction (PFC) and voltage regulation in a Z-source network (ZSN) can be introduced into the WPT system [109], which does not require additional power semiconductor devices or a control circuit. The control block diagram in Fig. 9 is employed for the H-Bridge for PFC. The ZSN is highly recommended for high-power requiring situations as it guarantees system reliability and additional boost features to the system, providing immunity to shoot-through states. The output voltage in the OBC with ZSN is regulated by using an active steady-state duty cycle (*D*act) as the control variable. The Z-source resonant-converter (ZSRC) is unaffected by shoot through states thereby improving the reliability of the system and the PFC is achieved by controlling the control variable shoot-through state duty cycle, obtained from the ZSRC at the shoot-through state. The system is experimentally tested for the power factor and THD which is found to be good at full load and the Power factor gets reduced from 0.987 to 0.957 with an increased THD value of 29.3% at half load condition requiring further modification in the control method to meet the necessary harmonic standard. The drawback of this system is that the efficiency is comparably low and at low converter output power, the input current is distorted with more THD.

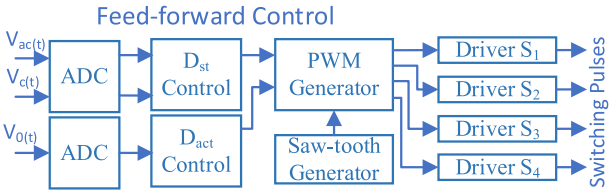

FIGURE 9. H-Bridge switching PWM control for resonant converter.

3) PHASE SHIFT CONTROL

The controller for achieving single-stage power conversion with a unity power factor for bidirectional WPT in Fig. 10 is

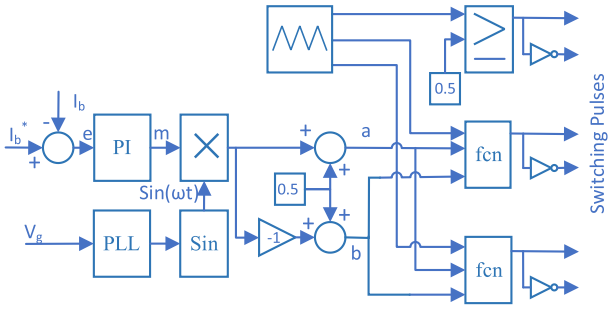

FIGURE 10. Phase shift control in bidirectional power converter.

proposed in [99] and is a simple method for easy implementation. By varying the phase shift angle and angle between the two phases of the converters, the power transferred to the primary coil and direction are controlled. By choosing a high value of filter capacity the ripple component found in the battery current which is double the track frequency can be eliminated. The additional functions such as buck, boost, or buck-boost operation are performed by appropriate selection of resonant tank characteristic impedance. From the investigational results it is observed that at low converter output, the input current is distorted. A high value of 0.99 PF is obtained for the 3.7KVA system in both G2V and V2G modes from simulation studies with the grid side THD 11.7% and 12.62% respectively. A prototype with 210W is developed to verify experimentally and the efficiency is found to deviate by around 5% from the simulation results.

4) OPTIMAL MODULATION CONTROL METHOD

In reducing the complexity of the circuit and to improve its efficiency, a new DAB converter has been proposed, which uses a 5th-order T-type CLCLC RIN. Resonant immittance network-based control is developed [110], which has the capability of wide output power level and wide voltage ratio operations. An optimum modulation method shown in Fig. 11 is developed to compute the phase shift parameters considering the loss model with a set of voltage ratio and output power level parameters. Various operating modes and their combinations are examined for the DAB converter with UPF, Soft Switching, Extended Phase-Shift and Dual Phase-Shift on the primary and secondary sides. To attain optimal efficiency

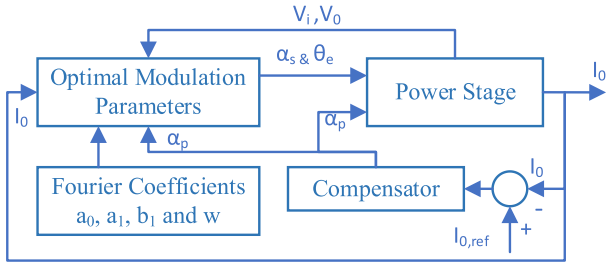

FIGURE 11. Optimal modulation control for DAB resonant immittance power converter.

under the set of specified parameters, with UPF operation, the circuit experiences hard switching and switching loss, and an increase in conduction loss due to the amplified circulating current during SS operation. The Efficiency under UPF operation is found to be less during low output current with a large value of circulating current.

5) OPTIMUM FREQUENCY TRACKING CONTROL

An additional converter in the WPT for voltage regulation and PFC results in the additional hardware. In [52], η.PF criterion is introduced for simplifying the WPT system considering the efficiency and power transfer capability. The system is then analyzed for sudden changes in the WPT coupling coefficient due to misalignments along the charging track in maximizing η.PF using the developed optimal frequency-tracking method which is depicted in Fig. 12 The phase-shift pulse width modulation technique is utilized to attain ZVS or ZCS with distinct values of duty cycle (D) and phase shift. The converter switching losses are minimized when chosen to work at the secondary resonant frequency. The UPF operating condition is achieved by making the input reactance zero or alternatively by controlling the normalized angular frequency to a unity value.

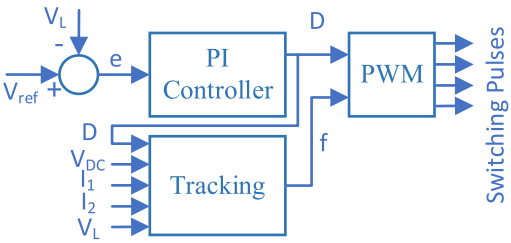

FIGURE 12. Optimum frequency tracking control for AC-DC WPT system.

6) TRIPLE PHASE SHIFT CONTROL

A new control scheme is developed in [111] to improve the efficiency of the DAB LCC resonant WPT converter with UPF operation by Triple Phase Shift PWM shown in Fig. 13. Phase shift applied to the primary converter regulates the DC Current/Voltage to the battery and applied to the secondary converter regulates the AC load resistance of the rectifier. Achievement of UPF operation of the DAB rectifier and inverter is contingent upon the phase angle deviation between the two converters. This angle is set to ensure optimal performance of the system. The symmetric structure of DAB is appropriate for the bi-directional action of WPT at a single resonant frequency. Setting up the inverter to rectifier phase shift angle as 90°, the UPF operation is achieved but only for the CC operation. During the CV operation in the process of obtaining the ZVS state, the phase shift angle is varied away from 90° and develops additional losses in the LCC circuit. The incorporation of wireless feedback for TPS closed-loop control implementation into the WPT system is a challenging part. The experimental outcomes for a 35W prototype show that the efficiency varies from 60 to 80% which is a low value

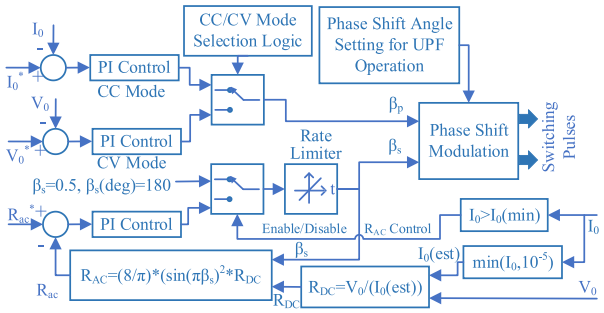

FIGURE 13. Triple phase shift control in DAB DC-DC resonant converter.

and for higher ratings the losses incurred become comparably low bringing the efficiency to a higher value.

7) IRREGULAR THREE-LEVEL ASYMMETRIC MODULATION AND PHASE-SHIFT MODULATION CONTROL

The single-stage matrix topology has some drawbacks like second-order frequency ripple in the battery side voltage or current and added switches count. To overcome the aforesaid drawbacks an integrated power stage WPT topology with bidirectional operation and power factor correction is implemented in a single-stage [112]. The modulation approach defined achieves simultaneous functions such as power factor correction for AC-DC, DC-DC wireless power transfer conversion, and soft-switching operation. This technique has the tendency to significantly improve the efficiency and dependability of power transfer systems. An irregular three-level symmetric modulation on the transmission side and phase-shift modulation on the other side are applied to achieve the desired functions. This topology implemented is shown in Fig. 14 exhibits several advantages such as a low switch count, soft switching implementation, lower THD, higher power factor and higher efficiency. A 500W test system is developed and tested for efficiency and THD with load values ranging from 20% to 100%. The test results at full rating give a very good power factor of 0.999 and a lower value of THD below 3.5%.

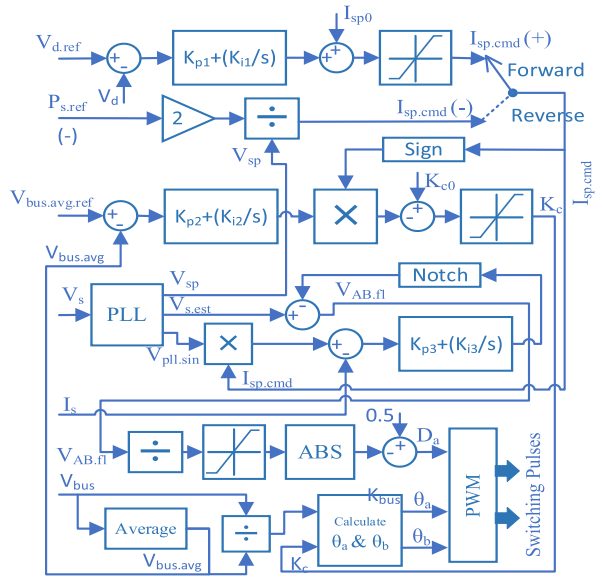

FIGURE 14. Irregular Three-Level asymmetric modulation and phase-shift modulation for bidirectional AC-DC WPT system.

8) SINUSOIDAL PULSE WIDTH MODULATION CONTROL

Reducing the switch count in the aspect of cost minimization is the main consideration in the article [113], hence a novel active power factor correction integrated 3-phase SSWPT converter is introduced with triple transmitter coils.

The rectification function of the PFC is achieved by utilizing the conventional three-phase PFC SPWM method, which is preferred due to its characteristic of possessing a fixed frequency. This method adopts two control loops one with PI for voltage regulation and the other with Proportional resonant (PR) for current control to execute PFC. The separate control loop does not affect the power quality of the circuit due to misalignments within the proper distance and the experimental efficiency and THD above half load yields a very good value. The full load efficiency and THD of this TPSSWPT developed for the 1.6KW system is 91.5% and 3.2% respectively. Fig. 15 shows the SPWM control adopted for PFC. A six-switch three-phase bridge structure on the input side provides the excitation for the WPT resonant tank circuit. Other than cost minimization the cohesive 3-phase WPT has the advantage of high input power quality with better efficiency.

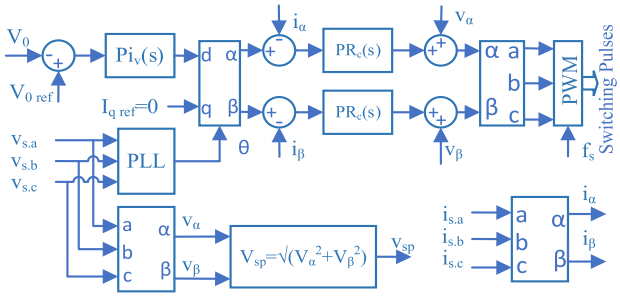

FIGURE 15. Sinusoidal pulse width modulation control for AC-DC WPT system.

9) THREE-LEVEL ASYMMETRIC MODULATION CONTROL METHOD

Without compromising the high performances of power factor correction and efficiency, a compact SSWPT converter is proposed in [114] with reduced semiconductor switches and diodes as well.

Compared with the conventional two-stage topologies, the drawbacks of diode bridge rectifier requirement and reduced quality of input power are eliminated by the use of compact AC-DC WPT converter and is a better alternative for the two-stage and recently developed single-stage converters employing two front-end diodes. The three-level asymmetric modulation method shown in Fig. 16 is implemented to achieve the PFC rectification with the three-loop control strategy for shaping AC current, maintaining constant supply

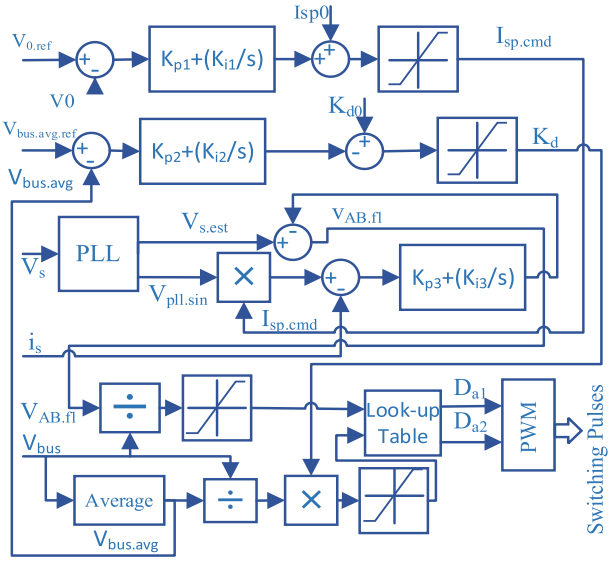

FIGURE 16. Three-Level asymmetric modulation control in SPSSWPT.

voltage and average bus voltage. A prototype of rating 500W employing this 3-level asymmetric modulation gives better efficiency at above half load condition and at 100% load reaches 91.8%. Also, the power factor and THD at full load are found to be almost unity and 2.66% respectively, which shows the enhancement of input power quality of the system with the proposed control method.

10) PHASE SHIFT MODULATION CONTROL METHOD

In [115] a single-stage bidirectional AC-DC topology is developed to eliminate the drawbacks such as ripple content of second order in the DC side of matrix-based converters with a new modulation technique shown in Fig. 17 employing PFC function, regulation and soft switching operation. The two components of AC-frequency and resonance-frequency components can be controlled separately for converter PFC achievement and primary-side WPT coil excitation, respectively. The concept involved here is the matching of instantaneous values of grid input power and converter output power. The simulation and practical implementation observations reveal the good performance of the methodology with an efficiency of 91.6% and a power factor of 0.999. The implemented topology offers many advantages, like reduced power device count, soft-switching process, and increased efficiency.

SUMMARY

The methodologies discussed for the power factor correction provide a better result only at a load value greater than half load which shows that there is a necessity for improvement for wide controllability operation. Table. 13 gives the comparison of the topologies employed for power factor correction with the achieved power factor values and compensation utilized in those methods. The additional PFC function incorporated in the SSWPT converter has little impact on

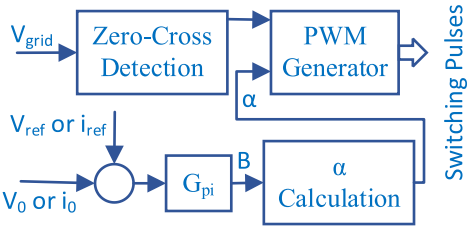

FIGURE 17. Phase shift modulation control for single-stage WPT converter.

the efficiency as it gets reduced while improving the power factor. As a fact in developing the charging infrastructure for EVs, increased charging stations create adverse effects if the quality of power is not maintained by the PFC techniques. The adverse effect of adding a PFC method in a single-stage converter increases the complexity of the control algorithm.

V. CHALLENGES IN SINGLE-STAGE WPT AND SCOPE FOR FUTURE WORK

Several Challenges arise in the implementation of single-stage converters for WPT which are enumerated and shown in Fig. 18.

A. COMPLY WITH CC, CV, AND CP PROFILE

The life of the EV battery depends on the charging profile selection during the battery charging process. The CC-CV charging process has the advantage of minimum wireless feedback requirement, but during load variations, the optimal load resistance varies and the charging process was not optimized properly for better efficiency. A dynamically supporting controller with a better response is required to achieve the CC charging process under load-varying conditions. In CC mode when misalignment arises the operation of the SSWPT converter for adjusting the current to a fixed value is similar to CV mode resulting in the complications of achieving better efficiency. Misalignment tolerant design of compensator and implementation provides efficiency improvement under anomalous situations. The variations in DC-link voltage must be reduced in order to reduce the difficulties that arise in the CC or CV charging process. Compared to the CC-CV process the CP-CV will be effective for the fast-charging process and is a difficult task in the realization of the battery charging process such as CC, CV and CP in the SSWPT.

B. CONTROL CIRCUIT COMPLEXITY

The major concern in the WPT is efficiency improvement and is employed with several techniques for achieving it. As the number of stages was reduced in the WPT to increase the efficiency the individual control applied in different stages needs to be applied in the single-stage alone which increases the complexity of the control method. In the case of an AC system, the initial stage of PFC is unavoidable in improving the power quality, thus adding further complexity to the

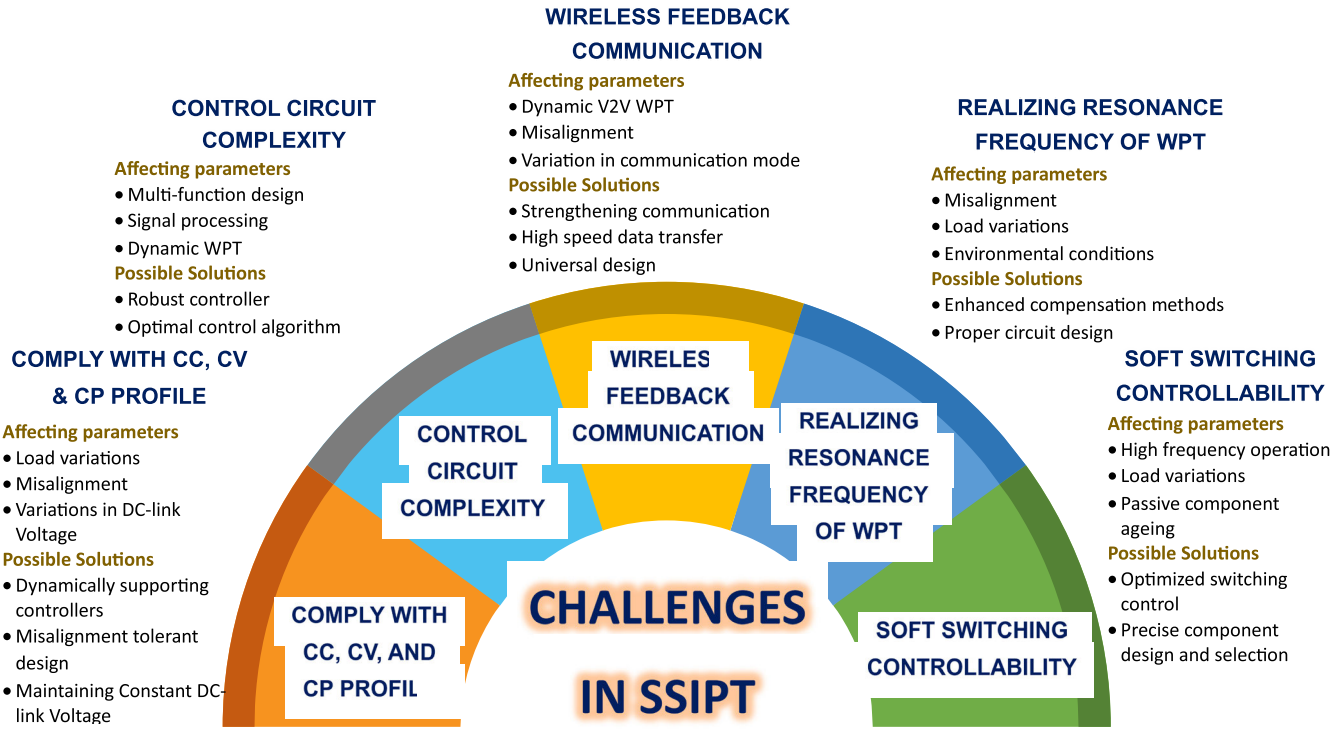

FIGURE 18. Challenges in single-stage wireless power transfer.

control method arises and it affects the efficiency of the SSWPT. Thus, a simple and robust controller needs to be designed capable of handling multiple functionalities. From the survey in the aspect of reducing complexity the space vector phase shift modulation suits for DAB converter in the control circuit. Further reducing switches, passive components and implementation of optimized controllers reduces the control complexity.

C. WIRELESS FEEDBACK COMMUNICATION

In some cases, feedback communication is not required and reduces the cost and size of the WPT as in the case of fixed frequency operation and independent control of the primary and secondary converter. Constant power operation tends to draw more input power at high misalignment conditions making the additional requirement of overcurrent protection in the converter primary side. As the complexity of the control circuit increases, feedback signals need to be sent to the off-board charging controller making the circuit less reliable by the inclusion of the wireless feedback communication and the implementation makes it challenging. The multi-coil WPT system necessitates additional parameters to be measured for control synthesis making the wireless communication further difficult. In the concept of dynamic power transmission wirelessly from vehicle to vehicle or other loads, more parameters are required to be processed, where communication needs to be strong enough to transfer the data with the required speed and accuracy.

D. REALIZING THE RESONANCE FREQUENCY OF WPT

For achieving good power transfer efficiency, the resonance phenomenon should be maintained in the WPT circuit and because of the coupling coil misalignment, load variations continuous control is a hard task but it should be adopted to achieve the same. In the dynamic environment frequency matching techniques should be adopted in the realization of the resonance in the SSWPT. The environmental conditions such as temperature variations, affect the coil characteristics, which should be compensated by suitable techniques for attaining resonance. Enhanced compensation methods such as hybrid compensation, adaptive compensation, load shift compensation and digital compensation assist in realizing the resonance frequency for the single-stage WPT.

E. SOFT SWITCHING CONTROLLABILITY

Whenever the switching frequency of the WPT converter is high the switching loss comes into the picture and needs to be considered for the WPT system. The ZVS method reduces switching loss and voltage stress in the converter switches. Achieving ZVS alone in the high-frequency converter is an easy task, but when other functionality such as PFC is added, the ZVS becomes difficult to achieve in the SSWPT system. The load variations also introduce the difficulty of soft switching implementation. Hence by proper design and selection of switches, inductive and capacitive components are required in handling the current and voltage stress on the switches with the consideration of EMI. An optimal

TABLE 13. Comparison of power factor correction topologies.

Control Block Diagram	Output Voltage	No. of Switches used	Efficiency	Compensation employed	Power Factor Achieved	Ref.
Resonant control technique	$V_0 = \sqrt{\frac{R_L(V_{Cr,max}^2 - V_{Cr,min}^2)}{2\pi Z_{LC}}}$	4	71-79	LC S	86-92	[108]
H-bridge switching PWM control	$V_0(t) = \frac{\lvert V_{ac}(t)\rvert}{\lvert k_{res}(\omega)\rvert(1-2D_{st(t)})}\sin\left(\frac{D_{act}(t)\pi}{2}\right)$	4	72.1	CLR SS	0.987	[109]
Phase Shift Control	$V_p = \lvert V_m sin(\omega_L(t))\rvert\frac{4}{\pi}\sum_{n=1,3,5\ldots}^{\infty}\frac{1}{n}\cos\left(n\omega_T t - \frac{n\delta_p}{2}\right)\times sin\left(\frac{n\delta_p}{2}\right)$	8	89.2 G2V 88.8 V2G	SS	0.99 G2V 0.99 V2G	[99]
Optimal modulation Control method	$V_s'(t) = \frac{4nV_s cos\alpha_s}{\pi}\sin(\omega_s t - \theta)$	8	97.1	CLCLC	Unity	[110]
Optimum Frequency Tracking control	$V_0 = \frac{V_{in}\omega MR}{\lvert Z_1 Z_2 + \omega^2 M^2\rvert}$	4	0.89-0.91 (K=.1) 0.76-0.78 (K=.05)	SS	0.85-0.99 (K=0.1) 0.65-0.99 (K=.05)	[52]
Triple Phase Shift Control	$V_{ac\_rec} = \frac{2\sqrt{2}}{\pi}Sin(\pi\beta_s).V_{dc\_rec}$	8	60-80	LCC	Unity	[111]
Irregular three-level asymmetric modulation and phase-shift modulation control	$V_{AB.fl} = \begin{cases} V_{sp}\sin(\omega_1 t) - \omega_1 L_{f2} I_{sp} Cos(\omega_1 t), & Forward\ power\ flow \\ V_{sp}\sin(\omega_1 t) - \omega_1 L_{f2} I_{sp} Cos(\omega_1 t), & Reverse\ power\ flow \end{cases}$	8	91.7	SS	0.999	[112]
Sinusoidal Pulse Width Modulation control	$\frac{V_0}{V_{bus}} = \frac{\sin(D_A\pi)}{2}\frac{M_{as}}{L_{ra}} + \frac{\sin(D_B\pi)}{2}\frac{M_{bs}}{L_{rb}} + \frac{\sin(D_c\pi)}{2}\frac{M_{cs}}{L_{rc}}$	6	91.5	LCC	Unity	[113]
Three-level asymmetric modulation control method	$V_0 = \frac{M}{L_1}\times\frac{Sin(D_{a1}\pi) + Sin(D_{a2}\pi)}{2} \times\sqrt{V_{bus.avg}^2 - \frac{P_0}{\omega_1 C_{bus}}Sin(2\omega_1 t)}$	4	91.8	LCC S	0.999	[114]
Phase shift modulation control method	$V_{inv}(t) = \frac{2\sqrt{2}}{\pi}\lvert\sqrt{2}.V_{grid}Sin(\omega_0 t)\rvert.Sin\frac{\alpha}{2}$	4	91.6	RC SS	0.999	[115]

switching control strategy is required in the case of achieving multifunctional capability.

F. FUTURE SCOPE

There are many interesting challenges present in the SSWPT design and implementation for EV charging. SSWPT has a wide opportunity in the multiport, dynamic environment, and communication enhancement. The multiport system is beneficial in developing charging infrastructures that have the capability of charging more EVs. In a dynamic environment managing coupling is a difficult task and by proper aligning and tracking methods coupling can be made effective. With efficiency and safety considerations several signals need to communicate between on-board and off-board devices and have the opportunity for the development of faster and secure communication without data loss. To reduce carbon footprint renewable sources can be included in making zero-emission vehicles, that are completely independent of grid power, which was generated from many sources including fossil fuels. SSWPT with the added benefit of reducing the power requirement from the grid for EV charging and providing grid support in times of peak demand. The harmonics associated with SPSSWPT are comparably higher than TPSSWPT, hence suitable controller is necessary which should eliminate the harmonics to a considerable extent.

VI. CONCLUSION

This article has reviewed and summarized various architectures of the single-stage converter employed currently for WPT in EV charging applications. In the WPT field, a considerable amount of research papers is available in various applications, but only a few papers are available for SSWPT specifying limited improvements, which indicates that there must be more research work to be carried out in that area to compete with the power handling capacity of the wired charging. The single-stage WPT is subdivided into AC and DC charging technologies and was discussed separately. Among the current works in literature, considering an

efficiency point of view the DC input WPT topology provides better efficiency and the absence of harmonics makes it still a worthwhile architecture. This simplest structure offers better controllability than the single-phase AC topologies. Integration with renewables in making emission-free charging centers can contribute to the net zero scenario. The TPSS-WPT topologies have less THD than the SPSSWPT and can be effectively used for high-power EV charging applications. To maintain power quality, it is essential to incorporate PFC in WPT systems, despite the resultant increase in control complexity. The implementation of a combination of Power Factor Correction (PFC) and Dual LCC compensation offers significant advantages in terms of enhanced efficiency and power quality. This viable solution can help optimize power quality management, thereby improving the overall system performance. Advancements in EV wireless charging technology and addressing the challenges in the right direction will ensure a safe and convenient system.

REFERENCES

[1] S. S. G. Acharige, M. E. Haque, M. T. Arif, N. Hosseinzadeh, K. N. Hasan, and A. M. T. Oo, "Review of electric vehicle charging technologies, standards, architectures, and converter configurations," *IEEE Access*, vol. 11, pp. 41218–41255, 2023, doi: 10.1109/ACCESS.2023.3267164.

[2] *Why We Need to Decarbonize Transportation | U.S. EPA*. Accessed: Oct. 14, 2023. [Online]. Available: https://www.epa.gov/greenvehicles/why-we-need-decarbonize-transportation

[3] S. M. Arif, T. T. Lie, B. C. Seet, S. Ayyadi, and K. Jensen, "Review of electric vehicle technologies, charging methods, standards and optimization techniques," *Electronics*, vol. 10, no. 16, p. 1910, Aug. 2021, doi: 10.3390/electronics10161910.

[4] R. Venugopal, C. Balaji, A. Dominic Savio, R. Narayanamoorthi, K. M. AboRas, H. Kotb, Y. Y. Ghadi, M. Shouran, and E. Elgamli, "Review on unidirectional non-isolated high gain DC–DC converters for EV sustainable DC fast charging applications," *IEEE Access*, vol. 11, pp. 78299–78338, 2023, doi: 10.1109/ACCESS.2023.3276860.

[5] J. Kumar and S. Kumar, "Standards for electric vehicle charging stations in India: A review," *Energy Storage*, vol. 4, no. 1, pp. 1–12, Feb. 2022, doi: 10.1002/est2.261.

[6] *Net Zero by 2050—Analysis—IEA*. Accessed: Sep. 10, 2023. [Online]. Available: https://www.iea.org/reports/net-zero-by-2050

[7] *Zero-Emission Vehicle Program | California Air Resources Board*. Accessed: Sep. 12, 2023. [Online]. Available: https://ww2.arb.ca.gov/our-work/programs/zero-emission-vehicle-program/about

[8] *Electric Vehicles—IEA*. Accessed: Sep. 10, 2023. [Online]. Available: https://www.iea.org/energy-system/transport/electric-vehicles#tracking

[9] M. Safayatullah, M. T. Elrais, S. Ghosh, R. Rezaii, and I. Batarseh, "A comprehensive review of power converter topologies and control methods for electric vehicle fast charging applications," *IEEE Access*, vol. 10, pp. 40753–40793, 2022, doi: 10.1109/ACCESS.2022.3166935.

[10] A. Sagar, A. Kashyap, M. A. Nasab, S. Padmanaban, M. Bertoluzzo, A. Kumar, and F. Blaabjerg, "A comprehensive review of the recent development of wireless power transfer technologies for electric vehicle charging systems," *IEEE Access*, vol. 11, pp. 83703–83751, 2023, doi: 10.1109/access.2023.3300475.

[11] A. Ahmad, M. S. Alam, and R. Chabaan, "A comprehensive review of wireless charging technologies for electric vehicles," *IEEE Trans. Transport. Electrific.*, vol. 4, no. 1, pp. 38–63, Mar. 2018, doi: 10.1109/TTE.2017.2771619.

[12] S. Thangavel, D. Mohanraj, T. Girijaprasanna, S. Raju, C. Dhanamjayulu, and S. M. Muyeen, "A comprehensive review on electric vehicle: Battery management system, charging station, traction motors," *IEEE Access*, vol. 11, pp. 20994–21019, 2023, doi: 10.1109/ACCESS.2023.3250221.

[13] Y. Shanmugam, P. Vishnuram, M. Bajaj, K. M. AboRas, and P. Thakur, "A systematic review of dynamic wireless charging system for electric transportation," *IEEE Access*, vol. 10, pp. 133617–133642, 2022, doi: 10.1109/ACCESS.2022.3227217.

[14] S.-C. Wang, G.-J. Chen, and Y.-H. Liu, "Adaptive charging strategy with temperature rise mitigation and cycle life extension for Li-ion batteries," *CPSS Trans. Power Electron. Appl.*, vol. 3, no. 3, pp. 202–212, Sep. 2018, doi: 10.24295/CPSSTPEA.2018.00020.

[15] *Trends in Charging Infrastructure—Global EV Outlook 2023—Analysis—IEA*. Accessed: Oct. 10, 2023. [Online]. Available: https://www.iea.org/reports/global-ev-outlook-2023/trends-in-charging-infrastructure

[16] D. Kim, A. Abu-Siada, and A. Sutinjo, "State-of-the-art literature review of WPT: Current limitations and solutions on IPT," *Electr. Power Syst. Res.*, vol. 154, pp. 493–502, Jan. 2018, doi: 10.1016/j.epsr.2017.09.018.

[17] H. S. Das, M. M. Rahman, S. Li, and C. W. Tan, "Electric vehicles standards, charging infrastructure, and impact on grid integration: A technological review," *Renew. Sustain. Energy Rev.*, vol. 120, Mar. 2020, Art. no. 109618, doi: 10.1016/j.rser.2019.109618.

[18] W. Liu, T. Placke, and K. T. Chau, "Overview of batteries and battery management for electric vehicles," *Energy Rep.*, vol. 8, pp. 4058–4084, Nov. 2022, doi: 10.1016/j.egyr.2022.03.016.

[19] *Free Access—NFPA 70: National Electrical Code*. Accessed: Sep. 11, 2023. [Online]. Available: https://link.nfpa.org/free-access/publications/70/2023

[20] *About NFPA 70, National Electrical Code? (NEC) | NFPA*. Accessed: Sep. 11, 2023. [Online]. Available: https://www.nfpa.org/NEC/

[21] H. Fathabadi, "Internal combustion engine vehicles: Converting the waste heat of the engine into electric energy to be stored in the battery," *IEEE Trans. Veh. Technol.*, vol. 67, no. 10, pp. 9241–9248, Oct. 2018, doi: 10.1109/TVT.2018.2854876.

[22] A. Gerlach, F. von Haeseler, H. Rottengruber, and R. Leidhold, "Nonlinear power control of an internal combustion engine without throttle actuator," *IEEE Trans. Control Syst. Technol.*, vol. 29, no. 4, pp. 1799–1806, Jul. 2021, doi: 10.1109/TCST.2020.3011263.

[23] E. A. Grunditz and T. Thiringer, "Performance analysis of current BEVs based on a comprehensive review of specifications," *IEEE Trans. Transport. Electrific.*, vol. 2, no. 3, pp. 270–289, Sep. 2016, doi: 10.1109/TTE.2016.2571783.

[24] L. Guo, B. Yang, and J. Ye, "Predictive energy management for dual-motor BEVs considering temperature-dependent traction inverter loss," *IEEE Trans. Transport. Electrific.*, vol. 8, no. 1, pp. 1501–1515, Mar. 2022, doi: 10.1109/TTE.2021.3116883.

[25] Q. Dong, D. Niyato, P. Wang, and Z. Han, "The PHEV charging scheduling and power supply optimization for charging stations," *IEEE Trans. Veh. Technol.*, vol. 65, no. 2, pp. 566–580, Feb. 2016, doi: 10.1109/TVT.2015.2399411.

[26] B. Jiang and Y. Fei, "A PHEV power management cyber-physical system for on-road applications," *IEEE Trans. Veh. Technol.*, vol. 66, no. 7, pp. 5797–5807, Jul. 2017, doi: 10.1109/TVT.2016.2642836.

[27] L. Tang, G. Rizzoni, and S. Onori, "Energy management strategy for HEVs including battery life optimization," *IEEE Trans. Transport. Electrific.*, vol. 1, no. 3, pp. 211–222, Oct. 2015, doi: 10.1109/TTE.2015.2471180.

[28] F. V. Cerna, M. Pourakbari-Kasmaei, M. Lehtonen, and J. Contreras, "Efficient automation of an HEV heterogeneous fleet using a two-stage methodology," *IEEE Trans. Veh. Technol.*, vol. 68, no. 10, pp. 9494–9506, Oct. 2019, doi: 10.1109/TVT.2019.2937452.

[29] J.-Y. Kim, B.-S. Lee, Y.-J. Lee, and J.-K. Kim, "Integrated multi mode converter with single inductor for fuel cell electric vehicles," *IEEE Trans. Ind. Electron.*, vol. 69, no. 11, pp. 11001–11011, Nov. 2022, doi: 10.1109/TIE.2021.3118390.

[30] S. Naresh, S. Peddapati, and M. L. Alghaythi, "A novel high quadratic gain boost converter for fuel cell electric vehicle applications," *IEEE J. Emerg. Sel. Topics Ind. Electron.*, vol. 4, no. 2, pp. 637–647, Apr. 2023, doi: 10.1109/JESTIE.2023.3248449.

[31] C. Panchal, S. Stegen, and J. Lu, "Review of static and dynamic wireless electric vehicle charging system," *Eng. Sci. Technol., Int. J.*, vol. 21, no. 5, pp. 922–937, Oct. 2018, doi: 10.1016/j.jestch.2018.06.015.

[32] K. Suresh, C. Bharatiraja, N. Chellammal, M. Tariq, R. K. Chakrabortty, M. J. Ryan, and B. Alamri, "A multifunctional non-isolated dual input-dual output converter for electric vehicle applications," *IEEE Access*, vol. 9, pp. 64445–64460, 2021, doi: 10.1109/ACCESS.2021.3074581.

[33] S. Harini, N. Chellammal, B. Chokkalingam, and L. Mihet-Popa, "A novel high gain dual input single output Z-quasi resonant (ZQR) DC/DC converter for off-board EV charging," *IEEE Access*, vol. 10, pp. 83350–83367, 2022, doi: 10.1109/ACCESS.2022.3195936.

[34] H. Heydari-doostabad and T. O'Donnell, "A wide-range high-voltage-gain bidirectional DC–DC converter for V2G and G2V hybrid EV charger," *IEEE Trans. Ind. Electron.*, vol. 69, no. 5, pp. 4718–4729, May 2022, doi: 10.1109/TIE.2021.3084181.

[35] V. Jain, S. Kewat, and B. Singh, "Three phase grid connected PV based EV charging station with capability of compensation of reactive power," *IEEE Trans. Ind. Appl.*, vol. 59, no. 1, pp. 367–376, Jan. 2023, doi: 10.1109/TIA.2022.3213530.

[36] G. Waltrich, M. A. M. Hendrix, and J. L. Duarte, "Three-phase bidirectional DC/DC converter with six inverter legs in parallel for EV applications," *IEEE Trans. Ind. Electron.*, vol. 63, no. 3, pp. 1372–1384, Mar. 2016, doi: 10.1109/TIE.2015.2494001.

[37] N. D. Dao, D.-C. Lee, and Q. D. Phan, "High-efficiency SiC-based isolated three-port DC/DC converters for hybrid charging stations," *IEEE Trans. Power Electron.*, vol. 35, no. 10, pp. 10455–10465, Oct. 2020, doi: 10.1109/TPEL.2020.2975124.

[38] R. Kushwaha and B. Singh, "Design and development of modified BL luo converter for PQ improvement in EV charger," *IEEE Trans. Ind. Appl.*, vol. 56, no. 4, pp. 3976–3984, Jul. 2020, doi: 10.1109/TIA.2020.2988197.

[39] V. Rathore, S. R. P. Reddy, and K. Rajashekara, "An isolated multilevel DC–DC converter topology with hybrid resonant switching for EV fast charging application," *IEEE Trans. Ind. Appl.*, vol. 58, no. 5, pp. 5546–5557, Sep. 2022, doi: 10.1109/TIA.2022.3168504.

[40] A. Elezab, O. Zayed, A. Abuelnaga, and M. Narimani, "High efficiency LLC resonant converter with wide output range of 200–1000 V for DC-connected EVs ultra-fast charging stations," *IEEE Access*, vol. 11, pp. 33037–33048, 2023, doi: 10.1109/ACCESS.2023.3263486.

[41] Md. R. Haque, K. M. A. Salam, and Md. A. Razzak, "A modified PI-controller based high current density DC–DC converter for EV charging applications," *IEEE Access*, vol. 11, pp. 27246–27266, 2023, doi: 10.1109/ACCESS.2023.3258181.

[42] D. Lyu, T. B. Soeiro, and P. Bauer, "Design and implementation of a reconfigurable phase shift full-bridge converter for wide voltage range EV charging application," *IEEE Trans. Transport. Electrific.*, vol. 9, no. 1, pp. 1200–1214, Mar. 2023, doi: 10.1109/TTE.2022.3176826.

[43] S. Mukherjee, J. M. Ruiz, and P. Barbosa, "A high power density wide range DC–DC converter for universal electric vehicle charging," *IEEE Trans. Power Electron.*, vol. 38, no. 2, pp. 1998–2012, Feb. 2023, doi: 10.1109/TPEL.2022.3217092.

[44] Y. Jiang, L. Wang, Y. Wang, J. Liu, M. Wu, and G. Ning, "Analysis, design, and implementation of WPT system for EV's battery charging based on optimal operation frequency range," *IEEE Trans. Power Electron.*, vol. 34, no. 7, pp. 6890–6905, Jul. 2019, doi: 10.1109/TPEL.2018.2873222.

[45] J. K. Nama, A. K. Verma, M. Srivastava, and P. S. Tomar, "An efficient inductive power transfer topology for electric vehicle battery charging," *IEEE Trans. Ind. Appl.*, vol. 56, no. 6, pp. 6925–6936, Nov. 2020, doi: 10.1109/TIA.2020.3018419.

[46] Y. Jiang, L. Wang, J. Fang, R. Li, R. Han, and Y. Wang, "A high-efficiency ZVS wireless power transfer system for electric vehicle charging WithVariable angle phase shift control," *IEEE J. Emerg. Sel. Topics Power Electron.*, vol. 9, no. 2, pp. 2356–2372, Apr. 2021, doi: 10.1109/JESTPE.2020.2984575.

[47] G. Li and H. Ma, "A hybrid IPT system with high-misalignment tolerance and inherent CC–CV output characteristics for EVs charging applications," *IEEE J. Emerg. Sel. Topics Power Electron.*, vol. 10, no. 3, pp. 3152–3160, Jun. 2022, doi: 10.1109/JESTPE.2021.3112969.

[48] N. Fu, J. Deng, Z. Wang, and D. Chen, "An LCC–LCC compensated WPT system with switch-controlled capacitor for improving efficiency at wide output voltages," *IEEE Trans. Power Electron.*, pp. 1–12, 2023, doi: 10.1109/TPEL.2023.3260207.

[49] J. Zhao, T. Cai, S. Duan, H. Feng, C. Chen, and X. Zhang, "A general design method of primary compensation network for dynamic WPT system maintaining stable transmission power," *IEEE Trans. Power Electron.*, vol. 31, no. 12, pp. 8343–8358, Dec. 2016, doi: 10.1109/TPEL.2016.2516023.

[50] T. Fujita, T. Yasuda, and H. Akagi, "A dynamic wireless power transfer system applicable to a stationary system," *IEEE Trans. Ind. Appl.*, vol. 53, no. 4, pp. 3748–3757, Jul. 2017, doi: 10.1109/TIA.2017.2680400.

[51] I. Karakitsios, F. Palaiogiannis, A. Markou, and N. D. Hatziargyriou, "Optimizing the energy transfer, with a high system efficiency in dynamic inductive charging of EVs," *IEEE Trans. Veh. Technol.*, vol. 67, no. 6, pp. 4728–4742, Jun. 2018, doi: 10.1109/TVT.2018.2816998.

[52] A. Zakerian, S. Vaez-Zadeh, and A. Babaki, "A dynamic WPT system with high efficiency and high power factor for electric vehicles," *IEEE Trans. Power Electron.*, vol. 35, no. 7, pp. 6732–6740, Jul. 2020, doi: 10.1109/TPEL.2019.2957294.

[53] G. Di Capua and N. Femia, "Optimal coils and control matching in wireless power transfer dynamic battery chargers for electric vehicles," *IEEE Access*, vol. 9, pp. 166542–166551, 2021, doi: 10.1109/ACCESS.2021.3129910.

[54] A. A. S. Mohamed, C. R. Lashway, and O. Mohammed, "Modeling and feasibility analysis of quasi-dynamic WPT system for EV applications," *IEEE Trans. Transport. Electrific.*, vol. 3, no. 2, pp. 343–353, Jun. 2017, doi: 10.1109/TTE.2017.2682111.

[55] M. S. Carmeli, F. Castclli-Dezza, M. Mauri, M. Rossi, A. Dolata, M. Pedretti, and I. Simonini, "Analysis of a quasi-dynamic wireless power transfer system for EV batteries charging," in *Proc. Int. Symp. Power Electron., Electr. Drives, Autom. Motion (SPEEDAM)*, Jun. 2018, pp. 383–388, doi: 10.1109/SPEEDAM.2018.8445238.

[56] O. C. O. M. Chinthavali, S. L. Campbell, and L. M. Tolbert, "Isolated wired and wireless battery charger with integrated boost converter for PEV applications," in *Proc. IEEE Energy Convers. Congr. Expo. (ECCE)*, Mar. 2015, pp. 607–614.

[57] Q. Deng, Y. Cheng, F. Chen, D. Czarkowski, M. K. Kazimierczuk, H. Zhou, and W. Hu, "Wired/wireless hybrid charging system for electrical vehicles with minimum rated power requirement for DC module," *IEEE Trans. Veh. Technol.*, vol. 69, no. 10, pp. 10889–10898, Oct. 2020, doi: 10.1109/TVT.2020.3019787.

[58] V.-B. Vu, J. M. González-González, V. Pickert, M. Dahidah, and A. Triviño, "A hybrid charger of conductive and inductive modes for electric vehicles," *IEEE Trans. Ind. Electron.*, vol. 68, no. 12, pp. 12021–12033, Dec. 2021, doi: 10.1109/TIE.2020.3042162.

[59] H. Karneddi and D. Ronanki, "A new hybrid conductive-inductive battery charger with reduced component count for electric transportation applications," in *Proc. IEEE Energy Convers. Congr. Expo. (ECCE)*, Feb. 2022, pp. 1–6, doi: 10.1109/ECCE50734.2022.9947764.

[60] A. T. L. Lee, W. Jin, S.-C. Tan, and S. Y. Hui, "Single-inductor multiple-output (SIMO) buck hybrid converter for simultaneous wireless and wired power transfer," *IEEE J. Emerg. Sel. Topics Power Electron.*, vol. 10, no. 2, pp. 2163–2177, Apr. 2022, doi: 10.1109/JESTPE.2020.3002987.

[61] H.-W. Jo, D. H. Sim, J.-A. Lee, W.-J. Son, and B. K. Lee, "Design and control of the adjustable turn-ratio LLC converter for high-efficiency operation of wired/wireless integrated EV charging system," in *Proc. Int. Power Electron. Conf.*, May 2022, pp. 2104–2110, doi: 10.23919/IPEC-Himeji2022-ECCE53331.2022.9806931.

[62] A. Rai, A. Singhal, and N. R. Tummuru, "PV-grid integrated hybrid charger for EV s with contactless and conductive charging capability," in *Proc. IEEE IAS Global Conf. Renew. Energy Hydrogen Technol. (GlobConHT)*, Mar. 2023, pp. 1–6, doi: 10.1109/GlobConHT56829.2023.10087749.

[63] Y. Zhang, Y. Wu, Z. Shen, W. Pan, H. Wang, J. Dong, X. Mao, and X. Liu, "Integration of onboard charger and wireless charging system for electric vehicles with shared coupler, compensation, and rectifier," *IEEE Trans. Ind. Electron.*, vol. 70, no. 7, pp. 7511–7514, Jul. 2023, doi: 10.1109/TIE.2022.3204857.

[64] Y. Wang, W. Ding, L. Huang, Z. Wei, H. Liu, and J. A. Stankovic, "Toward urban electric taxi systems in smart cities: The battery swapping challenge," *IEEE Trans. Veh. Technol.*, vol. 67, no. 3, pp. 1946–1960, Mar. 2018, doi: 10.1109/TVT.2017.2774447.

[65] T. Zhang, X. Chen, Z. Yu, X. Zhu, and D. Shi, "A Monte Carlo simulation approach to evaluate service capacities of EV charging and battery swapping stations," *IEEE Trans. Ind. Informat.*, vol. 14, no. 9, pp. 3914–3923, Sep. 2018, doi: 10.1109/TII.2018.2796498.

[66] X. Liu, T. Zhao, S. Yao, C. B. Soh, and P. Wang, "Distributed operation management of battery swapping-charging systems," *IEEE Trans. Smart Grid*, vol. 10, no. 5, pp. 5320–5333, Sep. 2019, doi: 10.1109/TSG.2018.2880449.

[67] H. Ko, S. Pack, and V. C. M. Leung, "An optimal battery charging algorithm in electric vehicle-assisted battery swapping environments," *IEEE Trans. Intell. Transp. Syst.*, vol. 23, no. 5, pp. 3985–3994, May 2022, doi: 10.1109/TITS.2020.3038274.

[68] A. A. Shalaby, M. F. Shaaban, M. Mokhtar, H. H. Zeineldin, and E. F. El-Saadany, "A dynamic optimal battery swapping mechanism for electric vehicles using an LSTM-based rolling horizon approach," *IEEE Trans. Intell. Transp. Syst.*, vol. 23, no. 9, pp. 15218–15232, Sep. 2022, doi: 10.1109/TITS.2021.3138892.

[69] M. O. Tarar, N. U. Hassan, I. H. Naqvi, and M. Pecht, "Techno-economic framework for electric vehicle battery swapping stations," *IEEE Trans. Transport. Electrific.*, vol. 9, no. 3, pp. 4458–4473, Oct. 2023, doi: 10.1109/TTE.2023.3252169.

[70] U. R. Prasanna, A. K. Singh, and K. Rajashekara, "Novel bidirectional single-phase single-stage isolated AC–DC converter with PFC for charging of electric vehicles," *IEEE Trans. Transport. Electrific.*, vol. 3, no. 3, pp. 536–544, Sep. 2017, doi: 10.1109/TTE.2017.2691327.

[71] A. Khaligh and M. D'Antonio, "Global trends in high-power on-board chargers for electric vehicles," *IEEE Trans. Veh. Technol.*, vol. 68, no. 4, pp. 3306–3324, Apr. 2019, doi: 10.1109/TVT.2019.2897050.

[72] A. Mahesh, B. Chokkalingam, and L. Mihet-Popa, "Inductive wireless power transfer charging for electric vehicles—A review," *IEEE Access*, vol. 9, pp. 137667–137713, 2021, doi: 10.1109/ACCESS.2021.3116678.

[73] G. Rituraj, G. R. C. Mouli, and P. Bauer, "A comprehensive review on off-grid and hybrid charging systems for electric vehicles," *IEEE Open J. Ind. Electron. Soc.*, vol. 3, pp. 203–222, 2022, doi: 10.1109/OJIES.2022.3167948.

[74] N. Tesla, "System of transmission of electrical energy," U.S. Patent 645 576, Mar. 20, 1900.

[75] Z. Zhang, H. Pang, A. Georgiadis, and C. Cecati, "Wireless power transfer—An overview," *IEEE Trans. Ind. Electron.*, vol. 66, no. 2, pp. 1044–1058, Feb. 2019, doi: 10.1109/TIE.2018.2835378.

[76] S. A. Q. Mohammed and J.-W. Jung, "A comprehensive state-of-the-art review of wired/wireless charging technologies for battery electric vehicles: Classification/common topologies/future research issues," *IEEE Access*, vol. 9, pp. 19572–19585, 2021, doi: 10.1109/ACCESS.2021.3055027.

[77] H. Zhou, J. Chen, Q. Deng, F. Chen, A. Zhu, W. Hu, and X. Gao, "Input-series output-equivalent-parallel multi-inverter system for high-voltage and high-power wireless power transfer," *IEEE Trans. Power Electron.*, vol. 36, no. 1, pp. 228–238, Jan. 2021, doi: 10.1109/TPEL.2020.3000244.

[78] Y. Zhang, S. Chen, X. Li, and Y. Tang, "Design of high-power static wireless power transfer via magnetic induction: An overview," *CPSS Trans. Power Electron. Appl.*, vol. 6, no. 4, pp. 281–297, Dec. 2021, doi: 10.24295/CPSSTPEA.2021.00027.

[79] X. Liu, F. Gao, Y. Zhang, M. M. Khan, Y. Zhang, T. Wang, and D. J. Rogers, "A multi-inverter high-power wireless power transfer system with wide ZVS operation range," *IEEE Trans. Power Electron.*, vol. 37, no. 12, pp. 14082–14095, Dec. 2022, doi: 10.1109/TPEL.2022.3195866.

[80] W. V. Wang, D. J. Thrimawithana, and M. Neuburger, "An Si MOSFET-based high-power wireless EV charger with a wide ZVS operating range," *IEEE Trans. Power Electron.*, vol. 36, no. 10, pp. 11163–11173, Oct. 2021, doi: 10.1109/TPEL.2021.3071516.

[81] C. Utschick, C. Som, J. Šouc, V. Große, F. Gömöry, and R. Gross, "Superconducting wireless power transfer beyond 5 kW at high power density for industrial applications and fast battery charging," *IEEE Trans. Appl. Supercond.*, vol. 31, no. 3, pp. 1–10, Apr. 2021, doi: 10.1109/TASC.2021.3056195.

[82] L. Wang, U. K. Madawala, J. Zhang, and M.-C. Wong, "A new bidirectional wireless power transfer topology," *IEEE Trans. Ind. Appl.*, vol. 58, no. 1, pp. 1146–1156, Jan. 2022, doi: 10.1109/TIA.2021.3097015.

[83] Y. Tang, Y. Chen, U. K. Madawala, D. J. Thrimawithana, and H. Ma, "A new controller for bidirectional wireless power transfer systems," *IEEE Trans. Power Electron.*, vol. 33, no. 10, pp. 9076–9087, Oct. 2018, doi: 10.1109/TPEL.2017.2785365.

[84] S. Samanta and A. K. Rathore, "A new inductive power transfer topology using direct AC–AC converter with active source current waveshaping," *IEEE Trans. Power Electron.*, vol. 33, no. 7, pp. 5565–5577, Jul. 2018, doi: 10.1109/TPEL.2017.2750081.

[85] H. Wang, U. Pratik, A. Jovicic, N. Hasan, and Z. Pantic, "Dynamic wireless charging of medium power and speed electric vehicles," *IEEE Trans. Veh. Technol.*, vol. 70, no. 12, pp. 12552–12566, Dec. 2021, doi: 10.1109/TVT.2021.3122366.

[86] Y. Huang, C. Liu, Y. Zhou, Y. Xiao, and S. Liu, "Power allocation for dynamic dual-pickup wireless charging system of electric vehicle," *IEEE Trans. Magn.*, vol. 55, no. 7, pp. 1–6, Jul. 2019, doi: 10.1109/TMAG.2019.2894163.

[87] P. Vishnuram, C. Balaji, T. Gono, T. Dockal, R. Gono, and P. Krejci, "A review on resonant inductive coupling pad design for wireless electric vehicle charging application," *Energy Rep.*, vol. 10, pp. 2047–2079, Nov. 2023, doi: 10.1016/j.egyr.2023.08.067.

[88] J. Rahulkumar., R. Narayanamoorthi., P. Vishnuram, M. Bajaj, V. Blazek, L. Prokop, and S. Misak, "An empirical survey on wireless inductive power pad and resonant magnetic field coupling for in-motion EV charging system," *IEEE Access*, vol. 11, pp. 4660–4693, 2023, doi: 10.1109/ACCESS.2022.3232852.

[89] W. Zhang and C. C. Mi, "Compensation topologies of high-power wireless power transfer systems," *IEEE Trans. Veh. Technol.*, vol. 65, no. 6, pp. 4768–4778, Jun. 2016, doi: 10.1109/TVT.2015.2454292.

[90] Y. Song, U. K. Madawala, D. J. Thrimawithana, and M. Vilathgamuwa, "Three-phase bi-directional wireless EV charging system with high tolerance to pad misalignment," *IET Power Electron.*, vol. 12, no. 10, pp. 2697–2705, Aug. 2019, doi: 10.1049/iet-pel.2018.6279.

[91] L. Tian, F. Yang, B. Cai, S. Li, K. Liu, and H. Zhao, "High misalignment tolerance in efficiency of WPT system with movable intermediate coil and adjustable frequency," *IEEE Access*, vol. 9, pp. 139527–139535, 2021, doi: 10.1109/ACCESS.2021.3117947.

[92] *J2954_202208: Wireless Power Transfer for Light-Duty Plug-in/Electric Vehicles and Alignment Methodology—SAE International*. Accessed: Sep. 17, 2023. [Online]. Available: https://www.sae.org/standards/content/j2954_202208/

[93] Z. Huang, S.-C. Wong, and C. K. Tse, "Design of a single-stage inductive-power-transfer converter for efficient EV battery charging," *IEEE Trans. Veh. Technol.*, vol. 66, no. 7, pp. 5808–5821, Jul. 2017, doi: 10.1109/TVT.2016.2631596.

[94] Z. Huang, C.-S. Lam, P.-I. Mak, S.-C. Wong, and C. K. Tse, "A single-stage inductive-power-transfer converter for constant-power and maximum-efficiency battery charging," *IEEE Trans. Power Electron.*, vol. 35, no. 9, pp. 8973–8984, Sep. 2020, doi: 10.1109/TPEL.2020.2969685.

[95] I.-W. Iam, I.-U. Hoi, Z. Huang, C. Gong, C.-S. Lam, P.-I. Mak, and R. P. D. S. Martins, "Constant-frequency and noncommunication-based inductive power transfer converter for battery charging," *IEEE J. Emerg. Sel. Topics Power Electron.*, vol. 10, no. 2, pp. 2147–2162, Apr. 2022, doi: 10.1109/JESTPE.2020.3004259.

[96] F. Xu, S.-C. Wong, and C. K. Tse, "Overall loss compensation and optimization control in single-stage inductive power transfer converter delivering constant power," *IEEE Trans. Power Electron.*, vol. 37, no. 1, pp. 1146–1158, Jan. 2022, doi: 10.1109/TPEL.2021.3098914.

[97] H. L. Li, A. P. Hu, and G. A. Covic, "A direct AC–AC converter for inductive power-transfer systems," *IEEE Trans. Power Electron.*, vol. 27, no. 2, pp. 661–668, Feb. 2012, doi: 10.1109/TPEL.2011.2159397.

[98] J. Liu, K. W. Chan, C. Y. Chung, N. H. L. Chan, M. Liu, and W. Xu, "Single-stage wireless-power-transfer resonant converter with boost bridgeless power-factor-correction rectifier," *IEEE Trans. Ind. Electron.*, vol. 65, no. 3, pp. 2145–2155, Mar. 2018, doi: 10.1109/TIE.2017.2745471.

[99] B. Vardani and N. R. Tummuru, "A single-stage bidirectional inductive power transfer system with closed-loop current control strategy," *IEEE Trans. Transport. Electrific.*, vol. 6, no. 3, pp. 948–957, Sep. 2020, doi: 10.1109/TTE.2020.3003749.

[100] J. Wang, C. Wang, S. Zhang, H. Yuan, Q. Zhang, and D. Li, "Constant-current and constant-voltage output using hybrid compensated single-stage resonant converter for wireless power transfer," *IEEE J. Emerg. Sel. Topics Power Electron.*, vol. 10, no. 5, pp. 6371–6382, Oct. 2022, doi: 10.1109/JESTPE.2022.3165179.

[101] S. Zhang, C. Wang, and D. Chen, "A single-stage wireless power transfer converter with hybrid compensation topology in AC input," *IEEE Trans. Veh. Technol.*, vol. 71, no. 8, pp. 8266–8279, Aug. 2022, doi: 10.1109/TVT.2022.3172363.

[102] C. Wang and J. Wang, "A hybrid LCC-SP compensation network with adjustable impedance angle used for single-stage wireless power transfer," *IEEE Trans. Transport. Electrific.*, vol. 9, no. 2, pp. 3452–3463, Nov. 2023, doi: 10.1109/TTE.2022.3222869.

[103] N. Xuan Bac, D. M. Vilathgamuwa, and U. K. Madawala, "A SiC-based matrix converter topology for inductive power transfer system," *IEEE Trans. Power Electron.*, vol. 29, no. 8, pp. 4029–4038, Aug. 2014, doi: 10.1109/TPEL.2013.2291434.

[104] M. Moghaddami, A. Anzalchi, and A. I. Sarwat, "Single-stage three-phase AC–AC matrix converter for inductive power transfer systems," *IEEE Trans. Ind. Electron.*, vol. 63, no. 10, pp. 6613–6622, Oct. 2016, doi: 10.1109/TIE.2016.2563408.

[105] A. K. Singh, E. Jeyasankar, P. Das, and S. K. Panda, "A single-stage matrix-based isolated three-phase AC–DC converter with novel current commutation," *IEEE Trans. Transport. Electrific.*, vol. 3, no. 4, pp. 814–830, Dec. 2017, doi: 10.1109/TTE.2016.2615811.

[106] J. Liu, W. Xu, K. W. Chan, M. Liu, X. Zhang, and N. H. L. Chan, "A three-phase single-stage AC–DC wireless-power-transfer converter with power factor correction and bus voltage control," *IEEE J. Emerg. Sel. Topics Power Electron.*, vol. 8, no. 2, pp. 1782–1800, Jun. 2020, doi: 10.1109/JESTPE.2019.2916258.

[107] C. S. Wong, J. Liu, L. Cao, and K. H. Loo, "A SWISS-rectifier-based single-stage three-phase bidirectional AC–DC inductive-power-transfer converter for vehicle-to-grid applications," *IEEE Trans. Power Electron.*, vol. 38, no. 3, pp. 4152–4166, Mar. 2023, doi: 10.1109/TPEL.2022.3220327.

[108] C.-K. Lee, S. Kiratipongvoot, and S.-C. Tan, "High-frequency-fed unity power-factor AC–DC power converter with one switching per cycle," *IEEE Trans. Power Electron.*, vol. 30, no. 4, pp. 2148–2156, Apr. 2015, doi: 10.1109/TPEL.2014.2330631.

[109] N. S. González-Santini, H. Zeng, Y. Yu, and F. Z. Peng, "Z-source resonant converter with power factor correction for wireless power transfer applications," *IEEE Trans. Power Electron.*, vol. 31, no. 11, pp. 7691–7700, Nov. 2016, doi: 10.1109/TPEL.2016.2560174.

[110] M. Yaqoob, K.-H. Loo, Y. P. Chan, and J. Jatskevich, "Optimal modulation for a fifth-order dual-active-bridge resonant immittance DC–DC converter," *IEEE Trans. Power Electron.*, vol. 35, no. 1, pp. 70–82, Jan. 2020, doi: 10.1109/TPEL.2019.2911233.

[111] Y. Cheong, S. Cao, R. T. Naayagi, and S. Lee, "Triple phase shift control of wireless charging DAB LCC resonant converter for unity power factor operation with optimized rectifier AC load resistance," *Appl. Sci.*, vol. 12, no. 22, p. 11871, Nov. 2022, doi: 10.3390/app122211871.

[112] J. Liu, F. Xu, C. Sun, and K. H. Loo, "A soft-switched power-factor-corrected single-phase bidirectional AC–DC wireless power transfer converter with an integrated power stage," *IEEE Trans. Power Electron.*, vol. 37, no. 8, pp. 10029–10044, Aug. 2022, doi: 10.1109/TPEL.2022.3156577.

[113] J. Liu, C. S. Wong, Z. Li, X. Jiang, and K. H. Loo, "An integrated three-phase AC–DC wireless-power-transfer converter with active power factor correction using three transmitter coils," *IEEE Trans. Power Electron.*, vol. 38, no. 6, pp. 7821–7835, Jun. 2023, doi: 10.1109/TPEL.2023.3238877.

[114] J. Liu, F. Xu, C. Sun, and K. H. Loo, "A compact single-phase AC–DC wireless power transfer converter with active power factor correction," *IEEE Trans. Ind. Electron.*, vol. 70, no. 4, pp. 3685–3696, Apr. 2023, doi: 10.1109/TIE.2022.3176297.

[115] W. Zhong, S. Bai, and C. Hu, "Power factor correction modulated wireless power transfer system with series-series compensation," *IEEE Access*, vol. 11, pp. 17576–17583, 2023, doi: 10.1109/ACCESS.2023.3244622.

D. PURUSHOTHAMAN received the bachelor's degree in electrical and electronics engineering from the Priyadarshini Engineering College, Tirupattur, in 2007, and the master's degree in power systems engineering from Anna University, India, in 2009. He is currently a Research Scholar with the Department of EEE, SRM Institute of Science and Technology, India. His research interests include electric vehicle, wireless power transfer, and optimization techniques.

R. NARAYANAMOORTHI (Member, IEEE) received the bachelor's degree in electrical engineering and the master's degree in control and instrumentation from Anna University, India, in 2009 and 2011, respectively, and the Ph.D. degree from the SRM Institute of Science and Technology, India, in 2019. He is currently an Associate Professor with the Department of Electrical and Electronics Engineering, SRM Institute of Science and Technology. His research interests include wireless power transfer, electric vehicle, power electronics, artificial intelligence, machine learning in renewable energy systems, and embedded system for smart sensors.

ALI ELRASHIDI has worked in academia for the past 23 years in various administrative and teaching roles, including the Associate Dean for Engineering of the College of Engineering, an Academic Consultant, and the Secretary of the Scientific Council, University of Business and Technology (UBT). He is currently a Professor with the Electrical Engineering Department, UBT. He was the PI or Co-PI for many funded research projects in the past ten years. His sponsors include ARDEC, USA, the Kuwait College of Science and Technology, and King Abdul Aziz University. He has published more than 65 research papers in national/international journals and conferences. He was a recipient of the Distinguished Assistant Professor of the Year Award of the University of Business and Technology, in 2015.

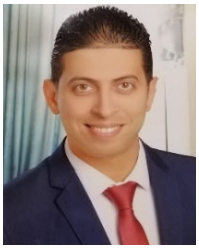

HOSSAM KOTB received the B.Sc., M.Sc., and Ph.D. degrees in electrical engineering from the Faculty of Engineering, Alexandria University, Alexandria, Egypt, in 2009, 2013, and 2020, respectively. His Ph.D. research work is focused on the performance enhancement of renewable energy conversion systems. He is currently an Assistant Professor with the Electrical Power and Machines Department, Faculty of Engineering, Alexandria University. His research interests include power system analysis, electrical drives, modern control techniques, smart grids, optimization, electric vehicles, and renewable energy systems. He is an Associate Editor of *Alexandria Engineering Journal* (AEJ).